AVIAN DIVERSIFICATION PATTERNS ACROSS THE K-PG BOUNDARY: INFLUENCE OF CALIBRATIONS, DATASETS, AND MODEL MISSPECIFICATION[1]

Daniel T. Ksepka[2] *and Matthew J. Phillips*[3]

ABSTRACT

Birds represent the most diverse extant tetrapod clade, with ca. 10,000 extant species, and the timing of the crown avian radiation remains hotly debated. The fossil record supports a primarily Cenozoic radiation of crown birds, whereas molecular divergence dating analyses generally imply that this radiation was well underway during the Cretaceous. Furthermore, substantial differences have been noted between published divergence estimates. These have been variously attributed to clock model, calibration regime, and gene type. One underappreciated phenomenon is that disparity between fossil ages and molecular dates tends to be proportionally greater for shallower nodes in the avian Tree of Life. Here, we explore potential drivers of disparity in avian divergence dates through a set of analyses applying various calibration strategies and coding methods to a mitochondrial genome dataset and an 18-gene nuclear dataset, both sampled across 72 taxa. Our analyses support the occurrence of two deep divergences (i.e., the Palaeognathae/Neognathae split and the Galloanserae/Neoaves split) well within the Cretaceous, followed by a rapid radiation of Neoaves near the K-Pg boundary. However, 95% highest posterior density intervals for most basal divergences in Neoaves cross the boundary, and we emphasize that, barring unreasonably strict prior distributions, distinguishing between a rapid Early Paleocene radiation and a Late Cretaceous radiation may be beyond the resolving power of currently favored divergence dating methods. In contrast to recent observations for placental mammals, constraining all divergences within Neoaves to occur in the Cenozoic does not result in unreasonably high inferred substitution rates. Comparisons of nuclear DNA (nDNA) versus mitochondrial DNA (mtDNA) datasets and NT- versus RY-coded mitochondrial data reveal patterns of disparity that are consistent with substitution model misspecifications that result in tree compression/tree extension artifacts, which may explain some discordance between previous divergence estimates based on different sequence types. Comparisons of fully calibrated and nominally calibrated trees support a correlation between body mass and apparent dating error. Overall, our results are consistent with (but do not require) a Paleogene radiation for most major clades of crown birds.

Key words: Aves, birds, divergence dating, fossils, paleontology, phylogeny.

One of the enduring debates in avian evolution centers around the timing of the crown radiation (Feduccia, 1995; Cooper & Penny, 1997; Cracraft, 2001; Ericson et al., 2006, 2007; Brown et al., 2007, 2008; Brown & van Tuinen, 2011; Mayr, 2013, 2014a). A straightforward interpretation of the fossil record of birds suggests that only a handful of deep divergences (i.e., Neognathae–Palaeognathae, Galloanserae–Neoaves, Anseriformes–Galliformes, Anhimidae–Anatoidea, and Anseranatidae–Anatidae splits) occurred during the Cretaceous, followed by an explosive radiation after the Cretaceous–Paleogene (K-Pg) extinction. This hypothesis is supported by the virtual absence of convincing Cretaceous crown bird fossils; only the anseriform (waterfowl) species †*Vegavis iaai* has been widely accepted as a Cretaceous crown bird (Clarke et al., 2005, though see Mayr, 2013). Other Cretaceous fossil birds either represent archaic taxa that clearly fall outside of the crown radiation or controversial taxa such as †*Teviornis* and †*Polarornis* that are too incomplete to place securely within the context of avian phylogeny (Clarke, 2004; Clarke & Norell, 2004; Mayr, 2004; Longrich et al., 2011). In contrast, most molecular divergence dating analyses have supported an extensive radiation of crown clade birds during the Cretaceous (e.g., Cooper & Penny, 1997; Brown et al., 2008; Pacheco et al., 2011; Haddrath & Baker, 2012; Jetz et al., 2012, though see Ericson et al., 2006; Jarvis et al., 2014). Indeed, some results suggest the basal crown divergences within individual orders such as Charadriiformes (shorebirds;

[1] We thank Peter Hoch and James Miller for organizing the 61st Annual Systematics Symposium and inviting this contribution; Robin M. Jones for graphic design support; and Kristin Lamm, N. Adam Smith, an anonymous reviewer, and editor Victoria Hollowell for constructive comments. This work was supported in part by a National Evolutionary Synthesis Center (NESCent) postdoctoral fellowship to D.T.K. and the NESCent Working Group "Synthesizing and Databasing Fossil Calibrations: Divergence Dating and Beyond" (National Science Foundation EF-0905606 and EF-0423641).

[2] Bruce Museum, Greenwich, Connecticut 06830, U.S.A. dksepka@brucemusuem.org.

[3] School of Earth, Environmental and Biological Sciences, Queensland University of Technology, Brisbane, QLD 4000, Australia. m9.phillips@qut.edu.au.

doi: 10.3417/2014032

ANN. MISSOURI BOT. GARD. 100: 300–328. PUBLISHED ON 10 AUGUST 2015.

Baker et al., 2007) and Psittaciformes (parrots; Wright et al., 2008) had already occurred during the Cretaceous, which would imply that many major crown bird morphotypes and ecotypes evolved alongside non-avian dinosaurs, ecologically diverse stem birds, and pterosaurs and also that an exceptionally large number of avian lineages survived the K-Pg extinction. Confounding matters, many fossil calibrations within Aves have been criticized as inappropriate due to stem/crown conflation and other issues (e.g., Mayr, 2005a; Ksepka, 2009; Wijnker & Olson, 2009; Smith, 2015). Likewise, many studies have used Cretaceous-age minimum calibrations based on the tectonic rifting of New Zealand from Australia for splits within clades such as Passeriformes (songbirds) and Palaeognathae (ratites and tinamous) (e.g., Cooper et al., 2001; Ericson et al., 2002; Barker et al., 2004). This calibration strategy rejects the possibility of dispersal by volant basal songbirds and the presumed volant ancestors of kiwi and moa and so may drive overestimates of divergence ages if biogeographic branching patterns in these clades reflect overwater dispersal rather than more ancient vicariance events (Phillips et al., 2010; Mayr, 2013; Worthy et al., 2013). This is cause for concern because the majority of clades that make up New Zealand's modern avifauna can be clearly shown to have arrived by long-distance dispersal (Trewick & Gibb, 2010). Beyond the prevalence of overwater dispersal, the complex geological history of the region makes assigning a precise date for the geological separation of New Zealand and Australia difficult, and the final severance of a close connection via the Lord Howe Rise may not have taken place until the Paleocene (Cande & Stock, 2004).

In many regards, the debate over the early crown radiation of birds parallels the debate over the early radiation of placental mammals. All potential Cretaceous crown placental fossils are controversial, and the fossil record suggests most major divergences occurred rapidly in the aftermath of the K-Pg extinction (Simpson, 1945; Archibald & Deutschman, 2001; Wible et al., 2007; O'Leary et al., 2013). In contrast, many molecular dates imply an expansive Cretaceous radiation for placental mammals (Springer et al., 2003; Bininda-Emonds et al., 2007; Meredith et al., 2011, though see Kitazoe et al., 2007; dos Reis et al., 2012). As with birds, some fossil calibrations have been critiqued as inaccurately placed, potentially leading to dating overestimates (Benton et al., 2009; Phillips et al., 2009; Phillips, in press.).

True divergence dates cannot be directly observed but are likely to lie somewhere between the minimum ages indicated by fossils and the extreme end of the molecular age estimate spectrum. Although the fossil record of birds is more complete than commonly portrayed, the material from the critical Late Cretaceous interval is both scarce and poorly represented, e.g., many isolated and/or fragmentary specimens (Olson, 1985; Mayr, 2009; Longrich et al., 2011). Beyond this preservation issue, there are challenges to identifying fossils on the deepest branches of the avian crown. Many closely related extant clades of birds are starkly different in morphology; it would presumably be difficult to recognize a fossil from a species lying on the stem lineage leading to a group such as Afroaves (a clade uniting such disparate groups as rollers, kingfishers, woodpeckers, hornbill, hawks, and owls) because of the lack of recognizable skeletal synapomorphies. Thus, the possibility remains that some poorly understood Cretaceous fossils could belong on deep branches within the avian crown but remain unrecognized as such. Nonetheless, it seems increasingly unlikely that crown members of extant orders such as Psittaciformes or Passeriformes have been overlooked in Cretaceous deposits.

Given the unobtainable nature of true divergence ages, it is productive to explore patterns of disparity between molecular divergence estimates and fossil ages in order to seek potential biases. One underappreciated phenomenon is that disparity between fossil ages and molecular dates tends to be proportionally greater for shallower nodes in the avian Tree of Life (Ksepka et al., 2014). This is counterintuitive from the perspective of fossil preservation and identification. All other factors being equal, the quality of the fossil record is expected to be higher for more recent time horizons than for older time horizons because more fossil-bearing rocks are preserved from younger deposits (Raup, 1972). Thus, one would expect rock preservation bias on average to contribute to greater disparity at deep nodes, rather than shallow nodes as observed. Likewise, identification bias (failure to properly identify the oldest fossil of a clade) may also contribute to greater disparity at deep nodes: if paleontologists fail to recognize the oldest fossil of a given clade, that clade's stratigraphic range will be artificially shortened. As mentioned above, fossils on deeper branches may be hard to identify, because it is not possible to predict a priori when in the history of the lineage each diagnostic trait evolved. In contrast, fossils occupying younger branches (e.g., divergences within crown families) should be relatively straightforward to identify: all diagnostic characters shared by the common ancestor of extant representatives

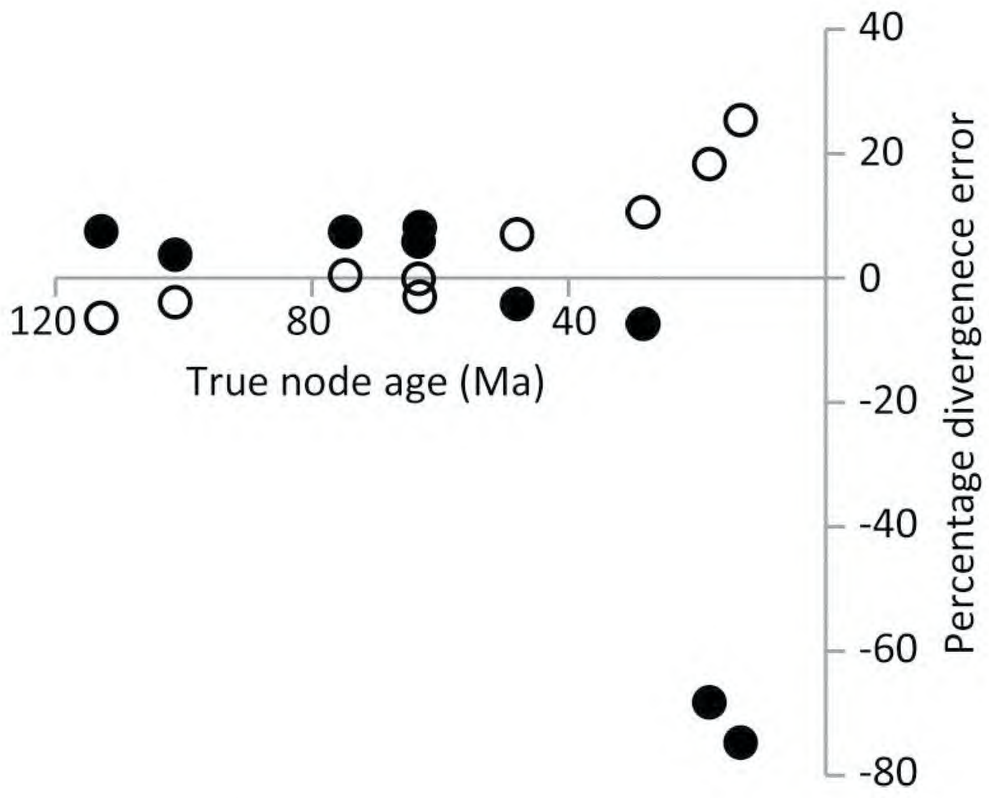


Figure 1. Divergence time errors (as a percentage of true node age) attributable to tree compression (open circles) and tree extension (closed circles) on a simulated 10-taxon tree pruned from the fully calibrated exon nDNA timetree. The horizontal axis represents divergence times simulated with the inferred alpha parameter for rate heterogeneity at 0.32. Tree compression was induced by undercorrecting for among-site rate heterogeneity (alpha = 2.0) and resulted in deep divergences being underestimated and shallow divergences overestimated. Tree extension was induced by overcorrecting for among-site rate heterogeneity (alpha = 0.1) and resulted in deep divergences being overestimated and shallow divergences underestimated. The horizontal scale indicates age as simulated in millions of years (Ma).

should be present in the oldest crown fossil. Although apomorphies of one of the two lineages branching from this common ancestor are technically required to prove crown status, paleontologists have tended to err in favor of assigning fossils to crown clades when the lack of such apomorphies leaves crown/stem status ambiguous. Conversely, loss of morphological features during fossilization can in some cases cause a specimen to erroneously appear in a more basal phylogenetic position, which could potentially lead to a crown taxon being misidentified as a stem taxon (Sansom et al., 2010, 2011; Sansom & Wills, 2013).

Another notable factor is that divergence dating analyses based on mitochondrial sequences have tended to yield older estimates than analyses based on nuclear sequences at least for ordinal level divergences (Ksepka et al., 2014). Clearly, both sets of dates cannot be correct, and some have considered mitochondrial dates problematic (van Tuinen & Hadly, 2004; Brown & van Tuinen, 2011). Thus, biases toward overestimation of mitochondrial DNA (mtDNA) dates and/or underestimation of nuclear DNA (nDNA) dates appear to exist in modeling substitution branch lengths, or in rate variation across the tree, at least at the ordinal level.

In sum, we contend that while biases in the fossil record are of major importance, they are unlikely drivers for many of the specific patterns of disparity observed across avian divergence dating studies. Therefore, exploration of potential drivers of disparity should also be sought among divergence dating analyses. One potential bias that has been widely discussed in relation to phylogeny is undercorrection or overcorrection for multiple nucleotide substitutions that occur at the same sites during the evolution of a lineage (e.g., Hendy & Penny, 1989; Siddall, 1998; Kolaczkowski & Thornton, 2004). Because this bias concerns underestimation or overestimation of branch lengths and becomes more pronounced more deeply in the tree, it will mislead divergence times. Branch-length underestimation leads to tree compression, with divergences that are shallower than calibrations being overestimated. Branch-length overestimation leads to tree extension, with divergences that are shallower than calibrations being underestimated. Both are illustrated in Figure 1 with analyses of simulated data and misspecification of substitution rate variation among sites.

Major sources of tree compression and extension suggested by Phillips (2009) included unaccounted-for rate heterogeneity among sites and substitution processes evolving across the tree (with models increasingly overcompensating for the amount of parallel changes between more divergent lineages). Although it is beyond the scope of this study to identify particular processes, a similar tree extension pattern might also be driven by alignment errors, which will manifest as increasing levels of branch-length overestimation as evolutionary depth increases and sequences become more difficult to align.

Several expectations are possible to derive here. One is that the higher saturation and heterogeneity of processes across substitution types in mtDNA versus nDNA (e.g., Wolfe et al., 1987; Hugall et al., 2007) provide greater potential for tree compression relative to nuclear sequences. However, that saturation and heterogeneity are greatly reduced by RY-coding (purines A+G → R, pyrmidines C+T → Y) and should reduce tree compression for mtDNA. If the potential for tree compression is sufficiently reduced, and if substitution processes evolve markedly across the tree, the balance may tip toward tree extension. In the case of birds (NT-coding predominates in most avian divergence dating analyses), such tree compression/tree extension artifacts may help explain at least some of the disparity observed between dates derived from nuclear and mitochondrial genes.

In this study, we examine patterns in avian molecular divergence estimation while controlling for phylogeny and aspects of the evolutionary models. Our aim is not to explicitly resolve avian divergence times, but rather to explore the influence of factors

such as gene type, the influence of single versus multiple calibrations relative to rate model alone, and relaxing the assumption of a molecular clock.

Materials and Methods

INSTITUTIONAL ABBREVIATIONS

The following abbreviations are used in this study: CM, Canterbury Museum, Christchurch, New Zealand; MACN, Museo Argentino de Ciencias Naturales Bernardino Rivadavia, Buenos Aires, Argentina; MGUH, Geological Museum of the University of Copenhagen, Denmark; MLP, Museo de La Plata, La Plata, Argentina; NHMUK, Natural History Museum, London, United Kingdom; NT, Tourment collection, Marseille, France; OCP.DEK/GE, Office Chérifien des Phosphates, Direction des Exploitations de Khouribga, Service Géologie, Khouribga, Morocco; PW, Landesamt für Denkmalpflege Rheinland-Pfalz, Mainz, Germany; QM, Queensland Museum, Brisbane, Queensland, Australia; SMF, Senckenberg Research Institute and Natural History Museum, Frankfurt am Main, Germany; SMNS, Staatliches Museum für Naturkunde, Stuttgart, Germany; USNM, National Museum of Natural History, Smithsonian Institution, Washington, D.C., U.S.A.

CALIBRATIONS

We utilized 15 node age priors (Appendix 1) that met recently proposed best practices for fossil calibrations (Parham et al., 2012). Several of these calibrations were discussed in greater detail by Ksepka and Clarke (2015) and Smith and Ksepka (2015). Each calibration was based on an individual fossil specimen that had been phylogenetically placed (assignable to the relevant node via either a published phylogenetic analysis or a set of apomorphies) and stratigraphically constrained so that the hard minimum age of the calibration corresponded to the minimum possible age of each calibrating specimen inclusive of geological dating error. We also specified maximum ages for each calibration based on global preservation patterns. Soft maxima are more subjective than hard minimum ages. In eight of our fossil calibrations, this greater uncertainty is accommodated by using an approximate lognormal distribution (i.e., a normal distribution truncated for the hard minimum at one standard deviation younger than the normal mean, with the soft maximum placed at the revised 2.5% upper bound). Such a distribution provides a wider region of high prior density, partly addressing one of the shortcomings of the lognormal distribution, while retaining the soft maximum, allowing 2.5% of the prior age distribution to surpass the maximum. In seven cases where the gap between our hard minimum and soft maximum ages is very wide and the fossil record cannot justifiably inform a prior distribution peak in the middle or either half of the distribution, we instead used uniform bounds. Uniform bounds are "hard" when used in the divergence analysis program, BEAST v.1.8.0 (Drummond & Rambaut, 2007). In addition to the fossil priors, a prior distribution for the root of the tree (basal split within Aves between Neognathae and Palaeognathae, node 1, Fig. 2) was specified with a hard minimum of 66.5 million years (Ma) and a soft maximum of 117.5 Ma, using a distribution that approximates the lognormal. This matches the root constraint used by Jetz et al. (2012).

MOLECULAR DATASET

Complete mitochondrial genome protein-coding DNA sequences (11,193 bp) and an 18-gene nuclear dataset comprising 7208 bp of protein-coding DNA (hereafter exon nDNA) and 14,691 bp of intron DNA (hereafter intron nDNA) and untranslated regions (UTRs) from Hackett et al. (2008) were aligned for a common set of 72 terminals. One additional gene (HMGN2) from Hackett et al. (2008) was excluded because it was missing for more than half of the taxa. All other genes were sampled at over 90% taxonomic completeness.

Taxa were selected to accommodate as many ordinal level clades as possible and to sample more densely within larger clades. In cases where loci were unavailable for a particular primary species, we included sequences from the closest available relative within either the genus or family (Appendix 2). This resulted in 21 cases where sequences from multiple species were combined into a composite terminal. Because different species provided the nuclear and mitochondrial sequences in many cases, a total of 142 species were sampled overall. Improved DNA matrix completeness can have substantial benefits in phylogenetic inference, while each member of the chimeric or composite taxon is theoretically equivalent for estimating phylogeny or divergence, so long as they form a clade relative to all other taxa in the matrix (Springer et al., 2004).

For the nDNA, we used the alignment of Hackett et al. (2008). For the mtDNA, automated alignment was performed in Muscle (Edgar, 2004a, 2004b) at EMBL (<http://www.ebi.ac.uk/Tools/msa/muscle/>) and then manually checked in Se-Al 2.0 (Rambaut, 1996). An important concern is the elevated mtDNA mutation rate, which amplifies both the impact of nucleotide composition biases and the difficulty of correcting for superimposed substitutions. As shown by Harrison et al. (2004), these problems are by far greatest at the largely synonymous third codon

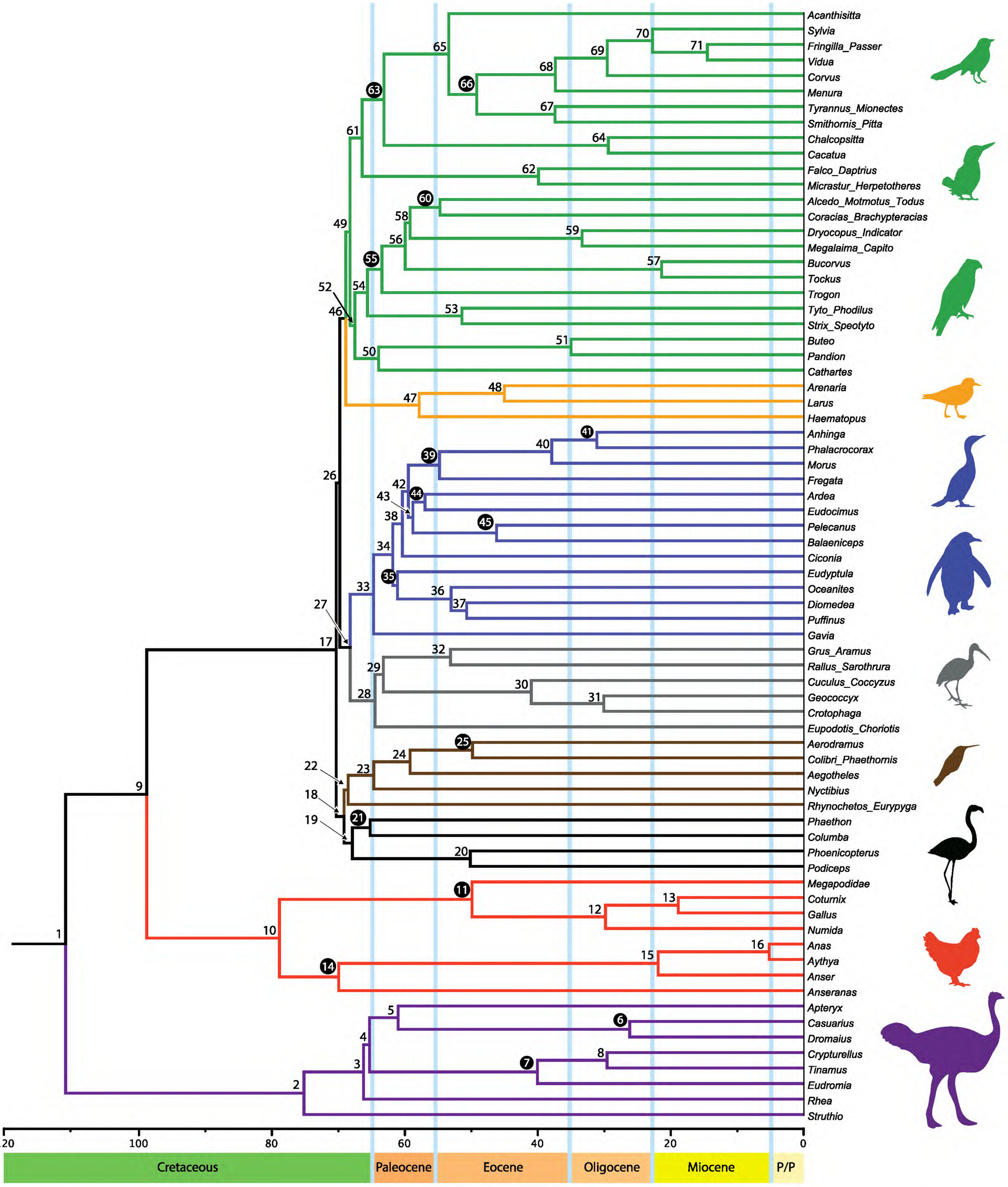


Figure 2. Timetree from divergence dating analyses using the preferred combined exon nDNA + RY-coded mtDNA dataset and applying all fossil calibrations. The horizontal scale below the diagram indicates age in millions of years, with dashed vertical lines indicating boundaries between geological time units. Node labels correspond to those in Tables 2–4 and Appendices 1 and 3. Filled circles indicate calibrated nodes.

positions, and so we excluded these from the mtDNA alignment. XML files containing the alignments, calibrations, and model settings are archived at Dryad (<doi:10.5061/dryad.3c3r3>).

ANALYSES

We estimated timescales for avian evolution using BEAST v.1.8.0 (Drummond & Rambaut, 2007) for both the nuclear exon and intron data and for the mitochondrial protein-coding data. The mtDNA was used as NT-coded (standard nucleotide sequence) or RY-coded to reduce phylogenetic signal erosion (see Phillips & Penny, 2003). Both the nuclear and mitochondrial protein-coding datasets were partitioned into codon positions. These partitioning schemes were preferred by the Bayesian information

Table 1. Partitioning schemes and substitution models.

Dataset	Partitions	Substitution model
NT mtDNA	codon positions	pos 1: GTR+I+G, pos 2: GTR+I+G
RY mtDNA	codon positions	pos 1: CF87+I+G, pos 2: CF87+I+G*
Exon nDNA	gene GC content × codon positions	low GC pos 1: TNR+I+G low GC pos 2: GTR+I+G low GC pos 3: GTR+G high GC pos 1: HKY+I+G high GC pos 2: GTR+I+G high GC pos 3: HKY+G
Intron nDNA	gene GC content	low GC: GTR+I+G high GC: GTR+I+G

Abbreviations: mtDNA, Mitochondrial DNA; nDNA, nuclear DNA.
* CF87+I+Γ4 (Cavender & Felsenstein, 1987) is the RY-coding equivalent to F81+I+Γ4.

criterion (in PartitionFinder 1.1.1, Lanfear et al., 2012) over concatenation or gene-wise partitioning. A combination of gene and codon partitioning was favored overall for the nuclear exons; however, with such high parameterization the analyses failed to converge. As a practical solution, we instead partitioned the nuclear genes into low and high GC content, which also tended toward low and high gamma distribution shape (alpha) parameters, respectively. Substitution model categories for each partition were assigned according to the most general of jModelTest (Posada, 2008) hierarchical likelihood ratio test (HLRT) and Akaike information criterion (AIC) recommendations (Table 1).

The same partitioning schemes were used for fully calibrated and nominally (root) calibrated relaxed clock analyses and for strict clock analyses. In the former cases, an uncorrelated relaxed clock model was used with rates among branches distributed according to a lognormal distribution, which can

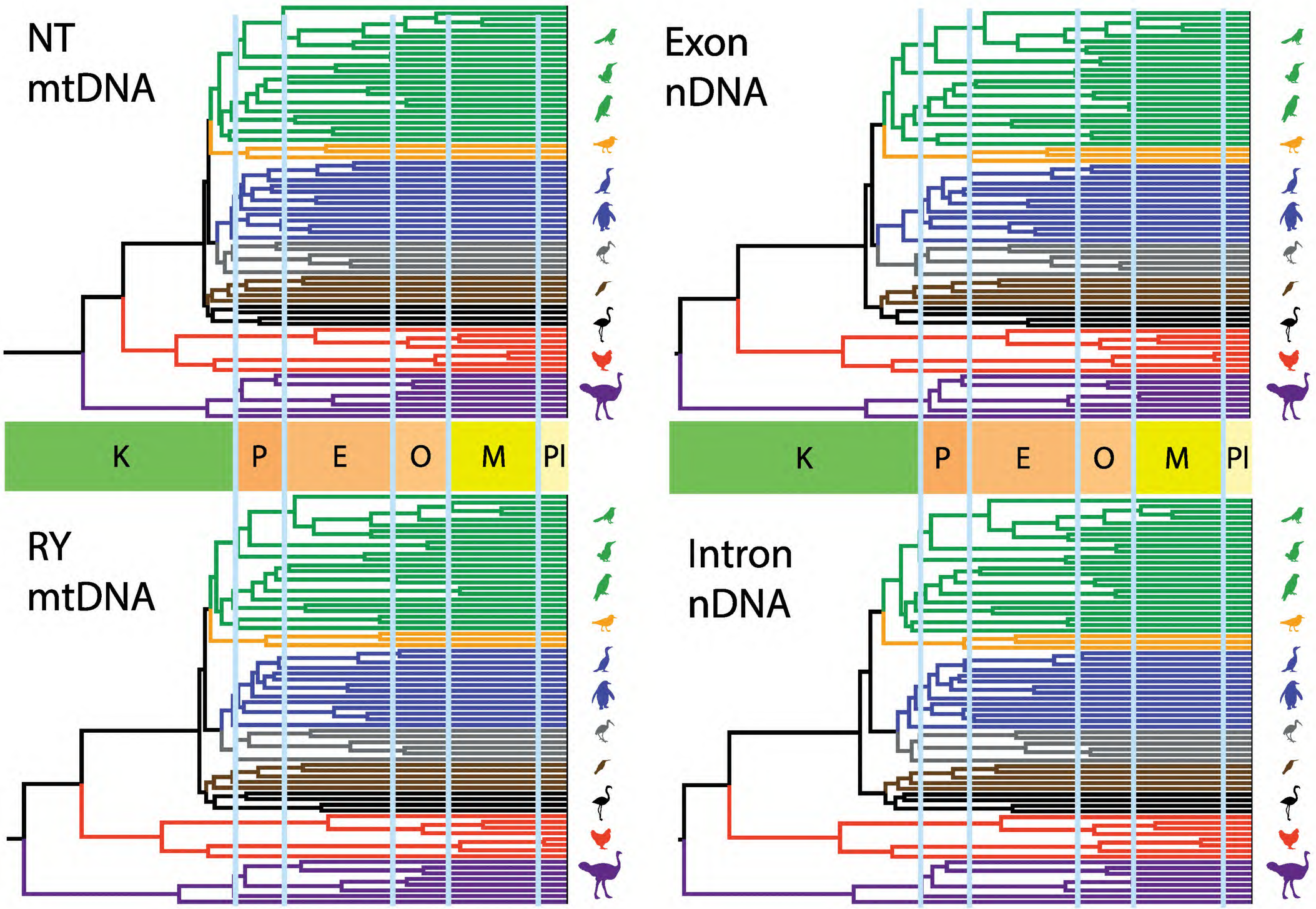


Figure 3. Timetrees from divergence dating analyses in BEAST with topology constrained and 15 fossil calibrations plus one root calibration applied comparing molecular datasets for NT- and RY-coding (A+G → R, C+T → Y) mtDNA as well as exon and intron/UTR nDNA.

Table 2. Median divergence age estimates (Ma) for all 71 nodes from fully calibrated divergence dating analyses. Combined analysis included coding nuclear DNA (nDNA) and RY-coded mitochondrial DNA (mtDNA). Node numbers correspond to those seen in Figure 2.

Node	Combined	Mitochondrial		Nuclear	
	Coding+RY	NT	RY	Exon	Intron
1. Aves (crown birds)	111.90	94.14	106.29	112.80	110.57
2. Palaeognathae (ratites and tinamous)	76.79	69.98	75.94	75.99	76.14
3. Notopalaeognathae (ratites excluding ostrich)	67.52	64.34	69.20	63.44	64.10
4. Tinamiformes/Novaeratitae	66.64	63.27	63.03	61.47	62.06
5. Novaeratitae (Apterygiformes [kiwi] + Casuariiformes)	62.39	56.65	52.06	56.94	59.13
6. Casuariiformes (cassowaries and emus)	26.36	29.96	28.10	28.07	28.46
7. Tinamiformes (tinamous)	40.02	45.53	44.13	35.96	35.59
8. *Crypturellus/Tinamus*	29.29	33.28	31.37	21.87	23.34
9. Neognathae (Galloanserae + Neoaves)	97.84	86.36	95.02	101.33	102.04
10. Galloanserae (Anseriformes + Galliformes)	78.47	75.99	79.31	80.59	80.39
11. Galliformes (landfowl)	49.41	48.96	46.78	48.03	49.13
12. Numididae (guineafowl)/Phasianidae (pheasants and allies)	29.91	30.97	28.24	29.63	30.73
13. *Gallus/Coturnix*	18.67	20.96	16.46	18.08	18.84
14. Anatoidea (magpie goose, ducks, and allies)	69.39	68.55	70.23	70.77	70.17
15. Anserinae (swans and geese)/other Anatidae	22.09	25.63	20.94	27.14	28.09
16. *Aythya/Anas*	5.16	11.44	4.52	7.01	9.45
17. Neoaves	70.41	70.61	71.96	76.11	76.44
18. Unnamed clade	69.24	69.89	70.65	72.98	71.76
19. Mirandornithes/other birds	68.40	68.94	68.97	69.79	69.90
20. Mirandornithes (Podicipediformes [grebes] + Phoenicopteriformes [flamingos])	50.05	59.81	48.08	43.91	45.66
21. Columbiformes (doves and pigeons)/Phaethontiformes (tropicbirds)	65.76	64.50	62.81	65.18	68.17
22. Eurypygiformes (kagu and subittern)/Strisores	68.65	69.04	69.12	71.18	69.34
23. Nyctibiidae (potoos)/Daedalornithes	64.81	65.90	65.55	66.45	66.96
24. Daedalornithes (Aegothelidae [owlet nightjars]/Apodiformes)	58.75	62.38	60.48	58.85	58.61
25. Apodiformes (swifts and hummingbirds)	49.71	51.31	51.72	49.68	50.04
26. Unnamed clade	69.88	69.76	70.89	74.80	74.47
27. Aequornithes (water birds)/other birds	68.32	68.05	67.62	73.65	69.24
28. Otidiformes (bustards)/other birds	64.64	66.57	65.07	66.12	66.56
29. Cuculiformes/Gruiformes	63.39	64.99	62.27	63.73	65.07
30. Cuculiformes (cuckoos)	41.75	50.05	42.45	39.30	44.36
31. *Geococcyx/Crotophaga*	30.94	42.10	31.83	25.63	31.88
32. Grues (cranes, trumpeters, and limpkin)/Rallidae (rails)	53.39	56.51	50.19	47.59	46.48
33. Aequornithes (waterbirds)	64.84	65.28	65.45	68.61	67.02
34. Austrodyptornithes/other Aequornithes	62.75	64.80	64.35	64.96	65.76
35. Austrodyptornithes (Sphenisciformes [penguins]+ Procellariiformes)	62.06	62.11	63.27	63.23	62.61
36. Procellariiformes (petrels and albatrosses)	53.68	55.63	45.64	47.63	56.41
37. *Puffinus/Diomedea*	51.36	50.06	39.11	42.78	54.35
38. *Ciconia*/other Aequornithes	61.34	63.42	61.59	63.62	63.14
39. Suliformes (frigatebirds, gannets, cormorants, and anhingas)	55.03	58.04	56.44	55.32	56.18
40. Sulidae (boobies and gannets)/Phalacrocoracoidea	38.32	48.57	40.88	39.16	38.40
41. Phalacrocoracoidea (cormorants and anhingas)	32.39	41.46	32.80	31.33	32.97
42. Suliformes/Pelecaniformes	59.67	62.93	60.53	60.79	61.52
43. Pelecaniformes (herons, ibises, pelicans, and allies)	58.99	61.21	59.20	59.45	58.92
44. Ardeidae (herons)/Threskiornithidae (ibises and spoonbills)	57.19	57.42	57.34	56.66	57.33
45. *Pelecanus/Balaeniceps*	46.52	48.79	42.98	43.91	43.09
46. Litoritelluraves (Charadriiformes + Telluraves)	68.98	69.31	69.78	72.42	71.92
47. Charadriiformes (shorebirds)	58.04	62.19	58.92	55.25	55.97
48. *Arenaria/Larus*	45.35	45.53	36.59	40.16	45.71
49. Telluraves (Afroaves + Australaves)	68.34	67.66	68.66	70.75	68.47
50. Cathartidae/Accipitres	64.48	65.66	64.51	61.81	66.31
51. *Buteo/Pandion*	35.42	45.53	36.70	31.35	36.12
52. Afroaves	67.63	67.18	67.62	68.66	67.50
53. Strigiformes (owls)	52.07	52.91	51.24	47.16	51.34
54. Strigiformes/Eucavitaves	66.14	65.22	65.34	66.42	65.64
55. Eucavitaves (Trogoniformes [trogons] + Picocoraciae)	63.60	62.28	61.57	63.35	63.79

Table 2. Continued.

Node	Combined	Mitochondrial		Nuclear	
	Coding+RY	NT	RY	Exon	Intron
56. Picocoraciae (Bucerotiformes + Picodynastornithes)	60.52	60.24	59.05	60.34	60.81
57. Bucerotiformes (hornbills)	22.33	31.28	20.99	23.93	27.17
58. Picodynastornithes (Coraciiformes + Piciformes)	59.02	58.66	56.94	58.66	58.02
59. Pici (woodpeckers and allies)	33.80	38.73	33.48	30.90	31.06
60. Alcedinidae (kingfishers)/Coracioidea (rollers and ground rollers)	54.97	54.57	54.41	54.27	53.16
61. Eufalconimorphae	66.94	64.21	64.44	68.66	64.79
62. Falconidae (falcons)	39.90	44.98	39.61	34.52	36.23
63. Psittacopasserae (Psittaciformes + Passeriformes)	63.70	62.77	62.14	62.19	62.60
64. Psittaciformes (parrots)	29.10	41.55	27.31	29.61	26.17
65. Passeriformes (songbirds)	53.66	55.23	53.33	52.51	51.45
66. Eupasseres (Tyranni + Passeri)	48.70	52.20	49.57	45.96	46.44
67. Tyranni (suboscine songbirds)	37.43	41.55	38.35	32.37	36.02
68. Passeri (oscine songbirds)	37.39	39.63	38.40	36.58	37.49
69. *Corvus*/other Passeri	29.27	31.47	29.00	28.40	28.29
70. *Sylvia*/*Vidua* + *Fringilla*	23.31	25.46	22.51	22.24	21.09
71. *Vidua*/*Fringilla*	14.35	16.50	12.86	13.30	15.08

provide greater flexibility than the exponential distribution option (Drummond et al., 2006). Birth–death tree priors were utilized for strict and relaxed clock analyses. The phylogeny of Hackett et al. (2008) was fixed for all analyses to ensure the comparability of divergence estimates from the alternative datasets and treatments.

Between two and 24 independent runs of 15 million Markov chain Monte Carlo (MCMC) generations were required for each analysis to provide estimated sample size values greater than 100 (as estimated in Tracer v1.5; Rambaut & Drummond, 2007) for all node height, prior, posterior, $-\ln L$, tree, and substitution parameters. Chains were sampled every 4000 generations after burn-ins of variable length, depending on convergence. We also conducted an analysis using a combined nuclear exon and RY-coded mtDNA dataset. We favor these datasets because RY-coding reduces compositional biases and phylogenetic signal erosion associated with the mtDNA (see above), and the nuclear intron data are expected to be the most susceptible to misalignment (see Morgan-Richards et al., 2008).

APPARENT DATING ERROR

In order to quantify the degree to which the fossil calibrations influence dates beyond providing a timescale, we compared the fully calibrated tree from each analysis to a scaled nominally calibrated tree based on the same underlying dataset. Each nominally calibrated tree used the same root calibration as the fully calibrated analyses, but excluded the other 15 fossil calibrations. We then scaled each nominally calibrated tree to minimize the sum of node height differences from the equivalent fully calibrated tree (e.g., multiplied all node dates from the nominally calibrated timetree by the single factor that results in the smallest overall difference in ages across all nodes between that nominally calibrated timetree and its fully calibrated equivalent). This scaling serves to counteract the possibility of any one divergence (such as the root) erroneously shifting the rest of the dates in one direction. Apparent dating error is equal to the difference in node ages between a fully calibrated tree and a presumably less accurate nominally calibrated tree (Phillips, in press). This provides a measure of how much a set of multiple calibrations informs the model of molecular rate variation and (presumably) corrects the relative dates given by relaxing the clock alone. We use the term "apparent dating error" for this measure because the true dates are, of course, unknown.

BODY MASS DATA

We collected average body mass data from the *CRC Handbook of Avian Body Masses* (Dunning, 2007), averaging data from multiple species in the case of composite taxa (Appendix 3). To test for an association between substitution rate misspecification and body mass, we compared log body mass to apparent dating error for nodes represented by pairs of tip taxa. Correlations between percent apparent dating error and log body mass for these nodes were evaluated using Pearson's product-moment correlation coefficient via the cor.test() function in R.

Table 3. Median divergence age estimates (Ma) for all 71 nodes from nominally calibrated divergence dating analyses. Node numbers correspond to those seen in Figure 2.

	Nominally Calibrated				Scaled Nominally Calibrated			
	Mitochondrial		Nuclear		Mitochondrial		Nuclear	
Node	NT	RY	Exon	Intron	NT	RY	Exon	Intron
1. Aves	81.31	81.08	81.20	80.86	94.89	122.27	139.34	121.21
2. Palaeognathae	61.24	53.45	48.54	50.86	71.47	80.60	83.29	76.24
3. Notopalaeognathae	56.46	44.74	39.94	41.75	65.89	67.47	68.54	62.58
4. Tinamiformes/Novaeratitae	55.59	42.93	38.81	40.27	64.87	64.74	66.60	60.36
5. Novaeratitae	49.12	31.24	35.82	38.10	57.32	47.11	61.47	57.11
6. Casuariiformes	18.50	4.88	7.54	10.76	21.59	7.36	12.94	16.13
7. Tinamiformes	41.01	30.06	21.88	23.69	47.86	45.33	37.55	35.51
8. *Crypturellus/Tinamus*	30.61	21.41	13.35	15.77	35.72	32.29	22.91	23.64
9. Neognathae	71.90	67.45	66.53	71.31	83.91	101.71	114.17	106.89
10. Galloanserae	59.20	51.79	49.18	53.10	69.09	78.10	84.39	79.60
11. Galliformes	48.22	39.69	37.43	42.12	56.27	59.85	64.23	63.14
12. Numididae/Phasianidae	30.08	21.86	21.27	25.30	35.10	32.96	36.50	37.92
13. *Gallus/Coturnix*	20.58	12.30	12.59	14.32	24.02	18.55	21.60	21.47
14. Anatoidea	47.17	36.98	37.66	39.51	55.05	55.77	64.62	59.23
15. Anserinae/other Anatidae	20.75	12.17	14.79	16.50	24.22	18.35	25.38	24.73
16. *Aythya/Anas*	9.11	2.94	3.91	6.32	10.63	4.43	6.71	9.47
17. Neoaves	61.11	49.03	44.35	51.70	71.32	73.94	76.10	77.50
18. Unnamed clade	60.53	47.35	42.07	49.03	70.64	71.40	72.19	73.50
19. Mirandornithes/other birds	59.64	46.02	40.60	48.00	69.60	69.40	69.67	71.95
20. Mirandornithes	50.24	29.97	26.61	31.37	58.63	45.19	45.66	47.02
21. Columbiformes/Phaethontiformes	55.61	39.82	38.41	47.15	64.90	60.05	65.91	70.68
22. Eurypygiformes/Strisores	59.60	45.82	41.14	47.15	69.55	69.10	70.60	70.68
23. Nyctibiidae/Daedalornithes	56.21	41.56	36.24	45.22	65.60	62.67	62.19	67.78
24. Daedalornithes	52.70	36.08	29.24	37.74	61.50	54.41	50.18	56.57
25. Apodiformes	40.39	26.22	20.23	30.00	47.14	39.54	34.71	44.97
26. Unnamed clade	60.35	48.23	43.59	50.13	70.43	72.73	74.80	75.14
27. Aequornithes/other birds	58.30	40.32	42.50	42.19	68.04	60.80	72.93	63.24
28. Otidiformes/other birds	56.77	38.42	38.16	40.38	66.25	57.94	65.48	60.53
29. Cuculiformes/Gruiformes	55.24	36.54	36.90	39.39	64.47	55.10	63.32	59.05
30. Cuculiformes	43.51	24.96	22.57	27.86	50.78	37.64	38.73	41.76
31. *Geococcyx/Crotophaga*	35.67	18.44	15.11	20.49	41.63	27.81	25.93	30.71
32. Grues/Rallidae	47.23	28.94	27.81	27.62	55.12	43.64	47.72	41.40
33. Aequornithes	52.72	34.96	32.82	39.85	61.52	52.72	56.32	59.74
34. Austrodyptornithes/other Aequornithes	52.16	33.47	27.52	38.72	60.87	50.47	47.22	58.04
35. Austrodyptornithes	47.55	32.12	25.90	35.11	55.49	48.44	44.44	52.63
36. Procellariiformes	40.98	23.96	19.94	30.46	47.82	36.13	34.22	45.66
37. *Puffinus/Diomedea*	36.49	20.59	17.62	29.10	42.58	31.05	30.24	43.62
38. *Ciconia*/other Aequornithes	50.96	30.42	26.58	36.69	59.47	45.87	45.61	55.00
39. Suliformes	46.37	26.18	20.31	31.18	54.11	39.48	34.85	46.74
40. Sulidae/Phalacrocoracoidea	38.61	18.40	13.80	21.40	45.06	27.75	23.68	32.08
41. Phalacrocoracoidea	32.93	14.10	10.48	18.08	38.43	21.26	17.98	27.10
42. Suliformes/Pelecaniformes	50.52	29.48	24.36	35.49	58.96	44.46	41.80	53.20
43. Pelecaniformes	48.90	27.99	23.42	33.43	57.07	42.21	40.19	50.11
44. Ardeidae/Threskiornithidae	44.27	25.67	20.75	32.22	51.66	38.71	35.61	48.30
45. *Pelecanus/Balaeniceps*	40.13	19.03	16.72	23.43	46.83	28.70	28.69	35.12
46. Litoritelluraves	60.01	47.69	42.59	48.49	70.03	71.92	73.08	72.69
47. Charadriiformes	53.15	36.74	31.97	36.84	62.03	55.40	54.86	55.22
48. *Arenaria/Larus*	39.18	22.09	23.99	30.50	45.72	33.31	41.17	45.72
49. Telluraves	58.84	47.15	41.90	46.26	68.67	71.10	71.90	69.34
50. Cathartidae/Accipitres	56.83	43.63	35.39	44.64	66.32	65.79	60.73	66.92
51. *Buteo/Pandion*	38.46	23.56	18.10	21.63	44.88	35.53	31.06	32.42
52. Afroaves	58.36	46.32	40.52	45.50	68.11	69.85	69.53	68.20
53. Strigiformes	44.05	33.28	26.41	32.66	51.41	50.19	45.32	48.96

Table 3. Continued.

Node	Nominally Calibrated				Scaled Nominally Calibrated			
	Mitochondrial		Nuclear		Mitochondrial		Nuclear	
	NT	RY	Exon	Intron	NT	RY	Exon	Intron
54. Strigiformes/Eucavitaves	56.38	44.50	39.24	43.96	65.80	67.11	67.34	65.90
55. Eucavitaves	53.64	41.30	37.67	42.40	62.60	62.28	64.64	63.56
56. Picocoraciae	51.41	38.11	34.66	39.27	60.00	57.47	59.48	58.87
57. Bucerotiformes	26.44	14.37	13.41	19.21	30.86	21.67	23.01	28.80
58. Picodynastornithes	49.66	35.44	33.20	36.25	57.95	53.44	56.97	54.34
59. Pici	32.52	21.22	16.79	18.94	37.95	32.00	28.81	28.39
60. Alcedinidae/Coracioidea	43.83	31.11	28.05	29.20	51.15	46.91	48.13	43.77
61. Eufalconimorphae	56.46	45.54	40.97	44.28	65.89	68.67	70.30	66.38
62. Falconidae	38.40	26.84	19.46	24.97	44.81	40.47	33.39	37.43
63. Psittacopasserae	55.49	44.69	38.07	43.07	64.76	67.39	65.33	64.56
64. Psittaciformes	30.11	17.98	17.75	15.85	35.14	27.11	30.46	23.76
65. Passeriformes	49.48	38.10	31.62	34.74	57.74	57.45	54.26	52.08
66. Eupasseres	46.98	35.38	27.43	31.47	54.83	53.35	47.07	47.17
67. Tyranni	37.25	26.61	18.81	24.29	43.47	40.13	32.28	36.41
68. Passeri	35.84	26.58	21.49	25.29	41.83	40.08	36.88	37.91
69. *Corvus*/other Passeri	28.61	20.06	16.47	19.73	33.39	30.25	28.26	29.58
70. *Sylvia*/*Vidua* + *Fringilla*	23.43	15.53	12.66	15.10	27.34	23.42	21.72	22.63
71. *Vidua*/*Fringilla*	15.50	8.75	7.65	10.91	18.09	13.20	13.13	16.35

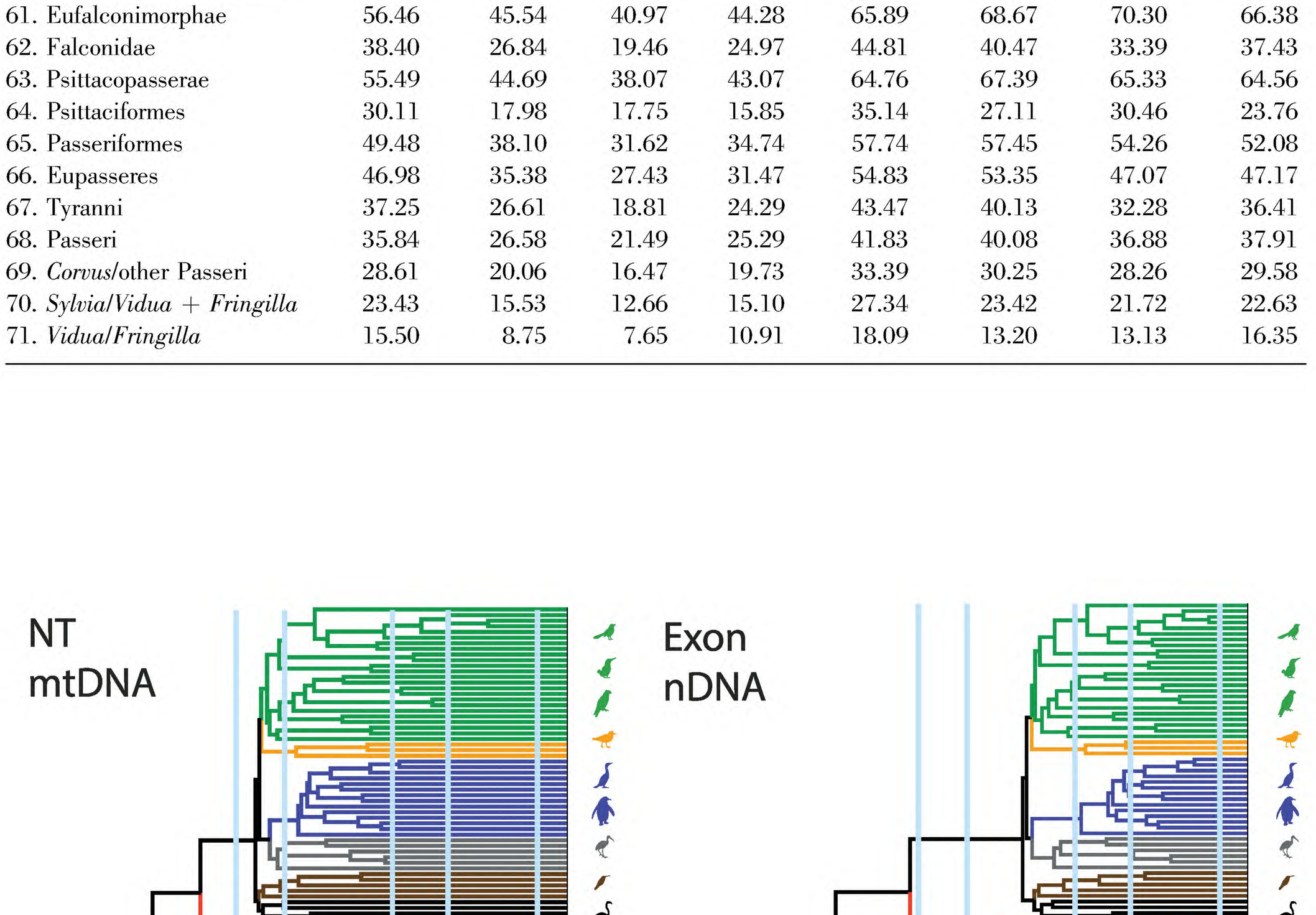


Figure 4. Nominally calibrated timetrees from divergence dating analyses in BEAST with topology constrained and only the root calibration applied. Molecular datasets correspond to those in Figures 3 and 5.

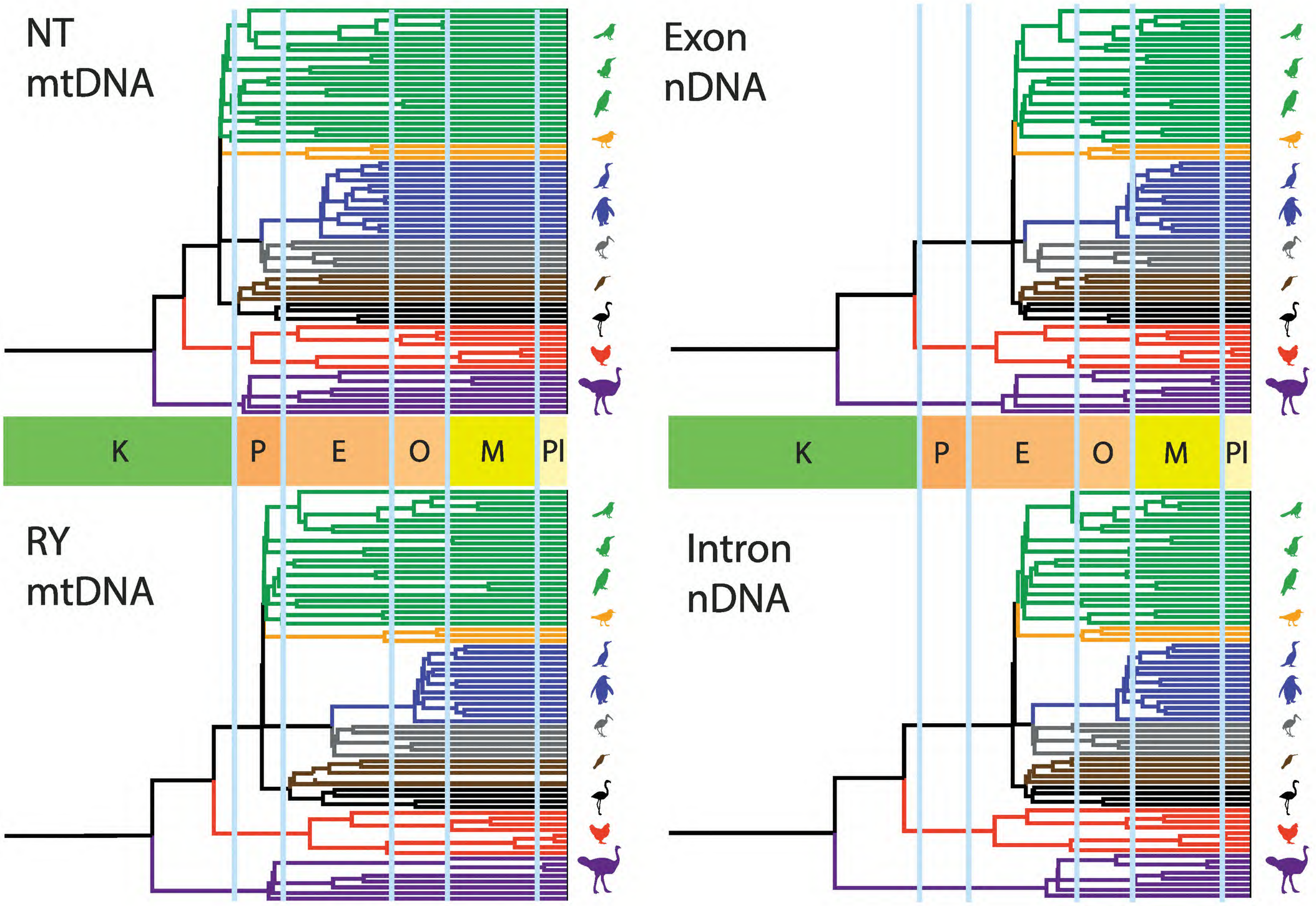


Figure 5. Timetrees from strict clock analyses. Molecular datasets correspond to those in Figures 3 and 4.

Table 4. Median divergence age estimates (Ma) for all 71 nodes from strict clock calibrated divergence dating analyses. Node numbers correspond to those seen in Figure 2.

	Strict Clock				Scaled Strict Clock			
	Mitochondrial		Nuclear		Mitochondrial		Nuclear	
Node	NT	RY	Exon	Intron	NT	RY	Exon	Intron
1. Aves	80.83	81.01	80.99	81.35	83.82	97.54	124.64	126.17
2. Palaeognathae	63.31	58.30	48.60	39.93	65.65	70.19	74.80	61.93
3. Notopalaeognathae	62.25	57.49	46.13	37.74	64.55	69.22	70.99	58.53
4. Tinamiformes/Novaeratitae	62.08	57.15	45.89	37.59	64.38	68.81	70.62	58.30
5. Novaeratitae	44.51	23.50	30.78	26.32	46.16	28.29	47.37	40.82
6. Casuariiformes	18.54	4.52	7.37	8.50	19.23	5.44	11.34	13.18
7. Tinamiformes	52.47	45.72	24.62	22.52	54.41	55.05	37.89	34.93
8. *Crypturellus/Tinamus*	46.06	39.76	17.16	17.16	47.76	47.87	26.41	26.62
9. Neognathae	75.02	69.01	65.86	67.81	77.80	83.09	101.36	105.17
10. Galloanserae	61.64	50.24	49.87	50.09	63.92	60.49	76.75	77.69
11. Galliformes	52.71	42.07	40.30	43.72	54.66	50.65	62.02	67.81
12. Numididae/Phasianidae	32.59	22.62	22.30	24.28	33.80	27.23	34.32	37.66
13. *Gallus/Coturnix*	25.48	15.01	16.27	16.94	26.42	18.07	25.04	26.27
14. Anatoidea	48.98	35.21	35.56	43.72	50.79	42.39	54.73	67.81
15. Anserinae/other Anatidae	20.96	10.29	13.47	24.28	21.74	12.39	20.73	37.66
16. *Aythya/Anas*	9.03	2.52	3.55	16.94	9.36	3.03	5.46	26.27
17. Neoaves	68.11	59.59	46.67	46.55	70.63	71.75	71.83	72.20
18. Unnamed clade	64.39	54.10	45.13	43.97	66.77	65.14	69.46	68.20
19. Mirandornithes/other birds	56.92	47.72	44.20	42.66	59.03	57.45	68.02	66.17
20. Mirandornithes	40.87	29.63	27.80	28.84	42.38	35.67	42.78	44.73
21. Columbiformes/Phaethontiformes	54.67	45.47	43.53	42.37	56.69	54.75	66.99	65.72
22. Eurypygiformes/Strisores	63.96	53.35	44.71	43.28	66.33	64.23	68.81	67.13
23. Nyctibiidae/Daedalornithes	61.33	49.56	42.18	42.43	63.60	59.67	64.92	65.81

Table 4. Continued.

Node	Strict Clock				Scaled Strict Clock			
	Mitochondrial		Nuclear		Mitochondrial		Nuclear	
	NT	RY	Exon	Intron	NT	RY	Exon	Intron
24. Daedalornithes	58.73	46.46	37.97	38.71	60.90	55.94	58.44	60.04
25. Apodiformes	48.25	40.24	32.17	35.02	50.04	48.45	49.51	54.32
26. Unnamed clade	67.95	59.37	46.48	46.15	70.46	71.48	71.53	71.58
27. Aequornithes/other birds	59.80	45.91	44.27	42.59	62.01	55.28	68.13	66.06
28. Otidiformes/other birds	59.17	45.48	41.61	42.30	61.36	54.76	64.04	65.61
29. Cuculiformes/Gruiformes	58.59	44.79	41.11	41.92	60.76	53.93	63.27	65.02
30. Cuculiformes	49.58	34.18	26.59	30.80	51.41	41.15	40.92	47.77
31. *Geococcyx/Crotophaga*	45.48	30.38	19.87	25.84	47.16	36.58	30.58	40.08
32. Grues/Rallidae	53.70	41.78	33.80	34.80	55.69	50.30	52.02	53.97
33. Aequornithes	48.21	29.81	26.14	26.07	49.99	35.89	40.23	40.43
34. Austrodyptornithes/other Aequornithes	47.73	29.17	24.19	24.76	49.50	35.12	37.23	38.40
35. Austrodyptornithes	44.76	28.12	22.10	21.13	46.42	33.86	34.01	32.77
36. Procellariiformes	39.68	21.68	17.54	18.02	41.15	26.10	26.99	27.95
37. *Puffinus/Diomedea*	36.78	20.10	15.28	16.67	38.14	24.20	23.52	25.86
38. *Ciconia*/other Aequornithes	43.25	28.28	23.79	24.21	44.85	34.05	36.61	37.55
39. Suliformes	44.87	26.99	20.19	21.63	46.53	32.50	31.07	33.55
40. Sulidae/Phalacrocoracoidea	40.10	21.81	15.37	16.19	41.58	26.26	23.65	25.11
41. Phalacrocoracoidea	36.57	19.92	13.68	15.07	37.92	23.98	21.05	23.37
42. Suliformes/Pelecaniformes	46.96	28.03	22.84	23.75	48.70	33.75	35.15	36.84
43. Pelecaniformes	41.95	21.17	22.26	22.81	43.50	25.49	34.26	35.38
44. Ardeidae/Threskiornithidae	38.65	26.23	21.20	22.28	40.08	31.58	32.63	34.56
45. *Pelecanus/Balaeniceps*	35.62	21.65	17.03	17.63	36.94	26.07	26.21	27.34
46. Litoritelluraves	67.89	59.25	46.18	45.52	70.40	71.34	71.07	70.60
47. Charadriiformes	50.88	35.69	31.63	32.86	52.76	42.97	48.68	50.97
48. *Arenaria/Larus*	38.26	25.46	26.78	29.15	39.68	30.65	41.21	45.21
49. Telluraves	67.78	59.16	46.00	44.63	70.29	71.23	70.79	69.22
50. Cathartidae/Accipitres	65.73	55.65	28.89	31.59	68.16	67.00	44.46	49.00
51. *Buteo/Pandion*	67.89	36.01	17.32	18.60	70.40	43.36	26.66	28.85
52. Afroaves	67.61	58.76	44.94	44.32	70.11	70.75	69.16	68.74
53. Strigiformes	60.66	52.78	30.92	33.03	62.90	63.55	47.59	51.23
54. Strigiformes/Eucavitaves	67.28	58.42	44.70	44.18	69.77	70.34	68.79	68.52
55. Eucavitaves	65.64	57.20	44.30	43.89	68.07	68.87	68.18	68.07
56. Picocoraciae	64.08	56.29	43.12	43.01	66.45	67.77	66.36	66.71
57. Bucerotiformes	32.05	15.37	15.53	18.41	33.24	18.51	23.90	28.55
58. Picodynastornithes	63.23	55.52	42.67	41.94	65.57	66.85	65.67	65.05
59. Pici	47.09	37.37	15.53	24.26	48.83	44.99	23.90	37.63
60. Alcedinidae/Coracioidea	58.50	53.26	39.61	38.06	60.66	64.13	60.96	59.03
61. Eufalconimorphae	66.64	58.79	45.77	44.03	69.11	70.78	70.44	68.29
62. Falconidae	50.27	39.61	23.35	23.70	52.13	47.69	35.94	36.76
63. Psittacopasserae	66.39	58.57	44.62	43.67	68.85	70.52	68.67	67.73
64. Psittaciformes	38.32	22.37	20.36	15.45	39.74	26.93	31.33	23.96
65. Passeriformes	62.28	52.34	37.35	34.90	64.58	63.02	57.48	54.13
66. Eupasseres	60.95	51.07	34.21	33.06	63.21	61.49	52.65	51.28
67. Tyranni	54.54	45.76	28.33	29.04	56.56	55.10	43.60	45.04
68. Passeri	44.56	36.90	26.87	26.62	46.21	44.43	41.35	41.29
69. *Corvus*/other Passeri	37.34	29.93	21.47	20.49	38.72	36.04	33.04	31.78
70. *Sylvia/Vidua* + *Fringilla_Passer*	33.47	26.50	18.60	17.10	34.71	31.91	28.63	26.52
71. *Vidua/Fringilla_Passer*	24.40	17.47	13.30	13.88	25.30	21.03	20.47	21.53

SIMULATION

The influence of tree compression and tree extension on divergence time estimates in otherwise controlled analyses was exemplified with data simulated on the fully calibrated exon nDNA timetree, pruned to 10 taxa, *Rhea* Brisson, *Dromaius* Vieillot, *Casuarius* Brisson, Megapodidae, *Coturnix* Garsault, *Gallus* Brisson, *Fringilla* L., *Vidua* Cuvier, *Eudyptula* Bonap., and *Diomedea* L. Seq-Gen 1.3.2 (Rambaut & Grassly, 1997) was used to simulate on the GTR+G model inferred for the original exon nDNA data, with branch lengths kept proportional to time and maintaining the overall tree length (in substitutions) for that 10-taxon subtree. Simulating under a strict clock for 20,000 nucleotide sites eliminates rate variation model errors as well as stochastic artifacts. Maximum likelihood (ML) analysis within PAUP* 4.0b10 (Swofford, 2002) under the simulated model accurately reconstructed the exon nDNA timetree.

As a simple means to producing tree compression and tree extension, additional ML reconstructions misspecified the shape of the gamma parameter (alpha). The value of alpha inferred from the exon nDNA was 0.32. This was increased to 2.0 to undercorrect for multiple substitutions at sites (saturation), resulting in tree compression. Alpha was reduced to 0.1 to overcorrect for multiple substitutions, resulting in tree extension. PAUP trees were uncalibrated, and so to compare differences in relative node heights between the treatments, each was scaled against the original 10-taxon exon nDNA tree to zero the sum of positive and negative node age differences.

Results

DIVERGENCE AGES

Analyses of the fully calibrated mtDNA and nDNA datasets all support a similar general pattern of survivorship across the K-Pg boundary (Figs. 2, 3, Table 2). Between 16 and 20 lineages among the sampled taxa are inferred to have diverged during the Cretaceous based on the median posterior node ages, though it is important to note two caveats. First, the 95% posterior probability range for most of these divergences overlaps the K-Pg boundary. Only six to eight lineages have highest posterior density (HPD) intervals that fall entirely within the Cretaceous. Second, and conversely, the number of K-Pg boundary-crossing lineages observed should be taken as a minimum estimate, as lineage birth–death processes would imply the existence of additional now-extinct lineages crossing as well.

The nominally calibrated analyses resulted in younger raw dates across the tree for all four molecular datasets (NT mitochondrial, RY mitochondrial, nuclear exons, and nuclear introns; Table 3, Fig. 4), with only three avian lineages (Palaeognathae, Galloanserae, and Neoaves) inferred to cross the K-Pg boundary. However, this is likely due to the combined influence of the single calibrated node and rate variation errors that the additional calibrations act to remedy. Scaling the nominally calibrated tree to minimize the sum of node height differences to the fully calibrated trees results in older node ages throughout the tree for all four molecular datasets (Table 3). This results in a similar number of lineages (16 to 18) inferred to have diverged during the Cretaceous as in the fully calibrated analyses.

Application of a strict clock model resulted in a modest shift relative to the fully calibrated dates for the NT mitochondrial dataset, with the average node age shifting by 7.98 Ma and 61% of node age estimates decreasing (Fig. 5). Progressively larger and more strongly negative shifts were noted in the RY mtDNA (13.68 Ma average shift, 86% decreasing), exon nDNA (20.74 Ma average shift, all decreasing), and intron nDNA datasets (21.14 Ma average shift, all but one decreasing). As with the nominally calibrated trees, scaling results in older node ages throughout the tree for all four molecular datasets (Tables 4, 5).

CODING, GENE TYPE, AND CALIBRATION STRATEGY COMPARISONS

Fully calibrated standard (NT) mtDNA data yielded significantly older ages on average for shallow nodes (nodes with median divergence ages from exon nDNA less than 66 Ma) than nuclear data ($P < 0.001$ for 2-tailed paired-sample *t*-test, though note these values may overstate significance due to non-independence of node age) (Fig. 6, Tables 2–4). Conversely, for deeper nodes (median divergence ages from exon nDNA > 66 Ma), the reverse was true and nuclear data yielded older ages than mitochondrial data ($P < 0.001$ for 2-tailed paired-sample *t*-test). These patterns are even more strongly expressed in the comparisons between the scaled nominally calibrated trees. Relatively little difference was noted between the dates from the exon nDNA and intron nDNA datasets for most nodes (Fig. 6).

Nucleotide coding regime for the mtDNA had a notable effect on divergence age estimates as well (Fig. 6). For shallow nodes (median divergence ages from RY mtDNA < 66 Ma), the NT-coded mtDNA dates were significantly older than those from the

Table 5. Number of avian lineages crossing the K-Pg boundary in the results of each analysis. The four molecular datasets include sequences for both NT- and RY-coded (A, G → R, C, T → Y) mitochondrial DNA (mtDNA) as well as translated exon and untranslated intron and nuclear DNA (nDNA).

Gene sequence datasets	Calibrations	Median posterior age Cretaceous	95% Posterior age distribution fully within Cretaceous
Exon nDNA + RY mtDNA	full	19	7
NT mtDNA	full	16	7
NT mtDNA	nominal	3	2
NT mtDNA	scaled nominal	16	—
NT mtDNA	strict clock	12	2
NT mtDNA	scaled strict clock	17	—
RY mtDNA	full	16	6
RY mtDNA	nominal	3	2
RY mtDNA	scaled nominal	17	—
RY mtDNA	strict clock	3	2
RY mtDNA	scaled strict clock	18	—
Exon nDNA	full	20	8
Exon nDNA	nominal	3	2
Exon nDNA	scaled nominal	18	—
Exon nDNA	strict clock	3	2
Exon nDNA	scaled strict clock	22	—
Intron nDNA	full	20	8
Intron nDNA	nominal	3	2
Intron nDNA	scaled nominal	18	—
Intron nDNA	strict clock	3	2
Intron nDNA	scaled strict clock	20	—

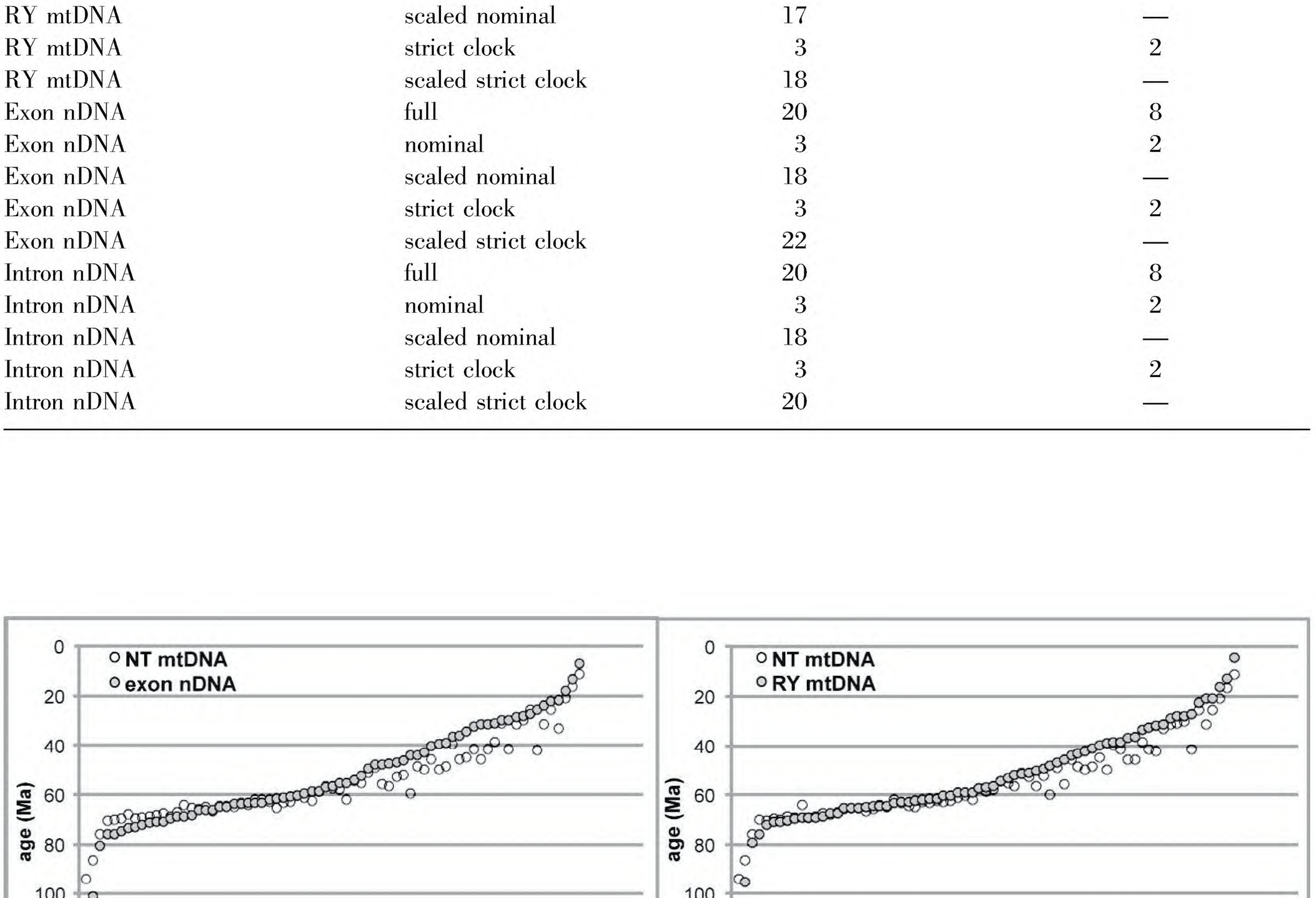


Figure 6. Comparisons of divergence estimates for all 71 nodes from analyses of NT-coded mtDNA, RY-coded mtDNA, exon nDNA, and intron nDNA. All graphs are from the analyses using the full fossil calibration set except for the bottom left, which is based on scaled, nominally calibrated analyses.

Table 6. Minimum sum of node height differences (Ma) between fully calibrated and scaled nominally calibrated trees. The four molecular datasets include sequences for both NT- and RY-coded (A, G → R, C, T → Y) mitochondrial DNA (mtDNA) as well as translated exon and untranslated intron nuclear DNA (nDNA).

Comparison	NT mtDNA	RY mtDNA	Exon nDNA	Intron nDNA
Fully calibrated to scaled nominally calibrated	169.5	406.2	401.1	294.7
Fully calibrated to scaled strict clock	550.9	761.4	573.4	609.9
Proportion of fully calibrated correction achieved by the relaxed clock model alone	0.69	0.47	0.30	0.52

RY-coded dataset ($P < 0.001$ for 2-tailed paired-sample *t*-test). Conversely, for deeper nodes (median divergence ages from RY mtDNA > 66 Ma), ages from NT-coded mtDNA were significantly younger than those from the RY-coded dataset ($P = 0.011$ for 2-tailed paired-sample *t*-test). Average difference between node age estimates is indeed greater between the RY mtDNA and NT mtDNA datasets than between the RY mtDNA and either the exon or intron nDNA dataset.

Average node age differences between fully and scaled nominally calibrated trees were lowest for the NT mtDNA dataset (Table 6). This indicates that the addition of the fossil calibrations results in more correction to the nDNA dates and the RY mtDNA dates than to the NT mtDNA dates. The overall proportion of correction from the strict clock offered by the calibrations compared to that obtained by relaxing the clock varies substantially. Relaxing the clock alone provides 69% of the overall fully calibrated correction for NT mtDNA but as little as 30% for the exon nDNA. The latter proportion is more similar to the 20% contribution of the relaxed clock model alone to correcting strict clock dates for (primarily) nuclear exon data among mammals (Phillips, in press).

A correlation between body mass and apparent dating error was detected. In each case but one, we reject the null hypothesis of no correlation between these variables at the 0.05 confidence level. No significant correlation was found for the NT mtDNA dataset. Body mass showed a significant correlation to apparent dating error in comparisons across all nodes representing pairs of tip taxa for the RY mtDNA, exon nDNA, and intron nDNA datasets (Fig. 7), with a tendency toward underestimation of node ages for larger-bodied clades.

Discussion

Patterns of disparity between datasets

A pronounced trend toward older dates in mitochondrial studies relative to nuclear studies has

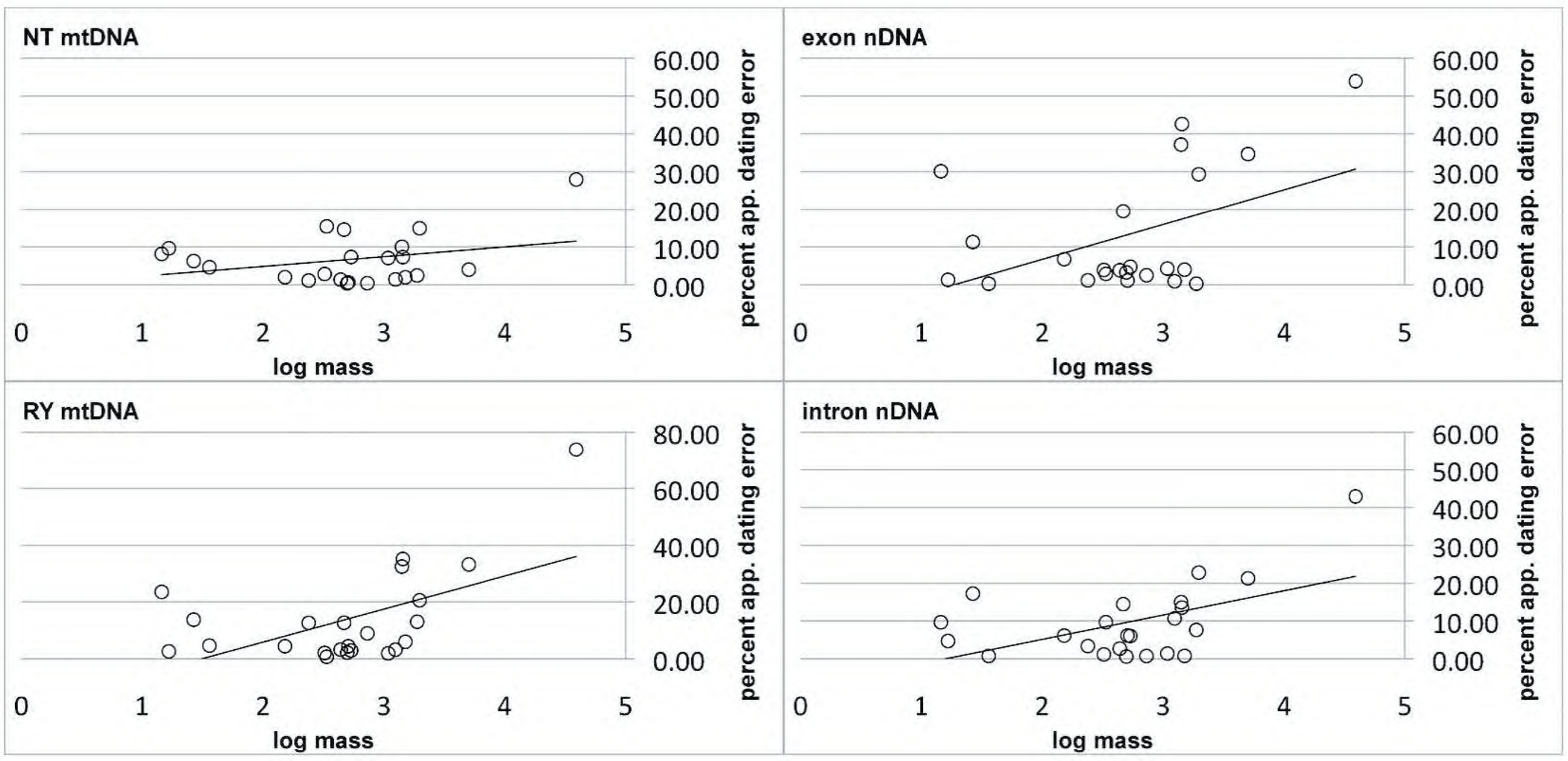


Figure 7. Apparent dating error (percentage node age difference between the fully calibrated tree and scaled nominally calibrated tree) as a function of log body mass for avian exemplars (Appendix 3). Each circle represents the node leading to a pair of tip taxa. NT mtDNA ($r^2 = 0.0966$, $P = 0.06758$), RY mtDNA ($r^2 = 0.3022$, $P = 0.003291$), exon nDNA ($r^2 = 0.2067$, $P = 0.01463$), and intron nDNA ($r^2 = 0.2714$, $P = 0.005398$) datasets.

Table 7. Extension-compression metrics for the fully calibrated relaxed clock trees. Correlation between the timetrees was tested for the difference between their paired node ages versus the average of those paired node ages. Corrected stemminess was estimated from the posterior distribution of branch lengths (substitutions.site^{-1}) in the BEAST analyses.

A. Timetree paired node age comparisons

Datasets	Spearman's rank correlation P value	Relatively extended component
NT mtDNA vs. RY mtDNA	< 0.0001	RY mtDNA
NT mtDNA vs. intron nDNA	< 0.0001	intron nDNA
NT mtDNA vs. exon nDNA	< 0.0001	exon nDNA
RY mtDNA vs. intron nDNA	$= 0.0701$	intron nDNA (not significant)
RY mtDNA vs. exon nDNA	< 0.0001	exon nDNA
Intron nDNA vs. exon nDNA	$= 0.0013$	exon nDNA

B. Corrected stemminess

	Mean	95% HPD
NT mtDNA	0.1459	0.1400–0.1518
RY mtDNA	0.2017	0.1903–0.2127
Intron nDNA	0.2336	0.2299–0.2373
Exon nDNA	0.2586	0.2493–0.2681

Abbreviations: HPD, Highest posterior density intervals; mtDNA, mitochondrial DNA; nDNA, nuclear DNA.

been observed in empirical comparisons of published avian divergence dates in one recent survey study (Ksepka et al., 2014). We observed older dates from analyses of NT mtDNA than from nDNA analyses for the majority of shallow nodes across the avian tree in the present study. However, deeper nodes exhibit the reverse pattern in our results. Because the 2014 survey study focused only on stem and crown divergences between ordinal level clades, it did not sample some of the very deep divergences, such as the Galloanserae–Neoaves split (Fig. 2, node 9), where older nuclear estimates prevail. Thus, the current results are consistent with broader patterns in the literature when sampling is taken into account.

Surprisingly, average node age differences between fully and scaled nominally calibrated trees are lowest for the NT mtDNA dataset (Table 6). This indicates that the addition of the 15 fossil calibrations exerts a larger degree of correction on the nDNA trees and the RY-coded mtDNA tree than on the NT-coded mtDNA tree. This is unexpected, as it is often presumed that standard mitochondrial data would be the most prone to branch length estimation error due to factors such as higher substitution rates and greater rate heterogeneity (Springer et al., 2001; Morgan et al., 2014). There are several possible explanations. The possibility cannot be discounted that the NT-coded mtDNA timetrees are the most accurate; the patterns of disparity with the other timetrees are consistent with tree extension operating in the nuclear and RY-coded mtDNA datasets. Alternatively, the relatively conservative maximum bounds of the calibration priors may be insufficiently informative to correct tree compression in the NT-coded mitochondrial dataset. A combination of these factors is also possible. If tree compression or extension underpins variation among timetrees, it is expected that the pairwise node age differences will depend on phylogenetic depth. Parametric tests make strong assumptions about the distribution of variation, and we instead used the non-parametric Spearman's rank correlation test. As shown in Table 7, correlations were highly significant ($P < 0.01$) for all comparisons between the four fully calibrated relaxed clock timetrees, except between the RY-coded mtDNA and the intron nDNA trees. A better indicator of relative tree compression/extension is the maximum likelihood (or Bayesian inference) corrected stemminess metric (Phillips & Penny, 2003), which is the proportion of overall tree length on internal branches. Stemminess has the statistical advantage of being based on independent branch lengths rather than potentially co-varying node ages. Tree compression and extension result in lower and higher stemminess, respectively. Corrected stemminess values (Table 7) are consistent with the timetree paired node age Spearman's rank correlation test. The pattern they confirm is that, relative to the other timetrees, the nuclear exon tree is the most extended (e.g., deep nodes relatively old, shallow nodes relatively young) and the NT-coded mtDNA tree is the most compressed (e.g., deep nodes relatively young, shallow nodes relatively old).

Life history variables potentially represent another important factor. Traits such as body mass and longevity may be strongly correlated to substitution rate and thus represent an important target for consideration in divergence dating studies. In mammals, the low substitution rate in large-bodied,

long-lived taxa relative to small-bodied, short-lived taxa has the potential to make a strong negative impact on the accuracy of inferred dates (Welch et al., 2008; Bromham, 2011; Lartillot & Delsuc, 2012; Phillips, 2015). Birds exhibit a less expansive range of body sizes (four orders of magnitude) than observed for mammals (eight orders of magnitude). Thus, body mass effects are predicted to be less influential on divergence dating results for birds. Our results suggest that body mass is correlated to apparent dating error, though to a lesser degree than observed in mammals. An important consideration here is that studies on mammals have suggested that longevity may be the driver of the relationship with evolutionary rate (Nabholz et al., 2008; Welch et al., 2008). The correlation between body size and evolutionary rate may in part be confounded by the correlation of body size with longevity. If body size is a poorer proxy for longevity in birds, then more data on longevity (and more calibrations) may eventually reveal a stronger relationship to apparent dating error than would be exposed by calibrating relaxed clocks. Likewise, future work may expand on this topic by comparing apparent dating error and life history variables across all nodes and by comparing calibrated nodes (where the correcting effect of calibrations is expected to be strongest) to uncalibrated nodes. We did not attempt comparisons sampling all nodes in the present study; this would require estimating ancestral body masses for nodes deeper in the phylogeny and the accuracy of such estimates would likely suffer greatly from lack of taxonomic sampling (e.g., approximately 1% of all living species).

Our results reaffirm the importance of multiple calibrations in informing clock models when dealing with heterogeneous rates (Waddell et al., 2001; Yang & Rannala, 2006). For example, the Sphenisciformes–Procellariiformes (penguin–petrel) split (Fig. 2, node 35) is recovered as 25.90–47.55 Ma in the nominally calibrated trees (44.44–55.49 Ma in the scaled nominally calibrated trees), whereas the fully calibrated tree yields substantially older dates (62.11–63.27 Ma) due to a 61 Ma minimum fossil calibration based on the oldest reported fossil penguin. Beyond this single calibrating fossil, thousands of older Paleogene penguin specimens are known from throughout the Southern Hemisphere, leaving no doubt that the uncalibrated divergence date is a severe underestimate. Because penguins and many procellariiforms are relatively long-lived, large-bodied birds, this may seem a case of life history traits influencing inferred substitution rates. The associated possibility of parallel rate deceleration in both lineages would provide a particularly difficult scenario for current rate models. However, deeper investigations are warranted before ascribing this explanation, as high levels of apparent age underestimation also can be detected at a few nodes that represent smaller-bodied clades. For example, the Apodidae–Trochilidae (hummingbird–swift) split (Fig. 2, node 25) represents the divergence between two of the smallest-bodied avian clades and is recovered as 20.23–40.39 Ma in age in the nominally calibrated trees (34.71–47.14 Ma in the scaled nominally calibrated trees). The fully calibrated tree yields older dates (49.68–51.72 Ma).

AVIAN EVOLUTION AND THE K-PG BOUNDARY

Our favored analyses (fully calibrated RY-mtDNA + exon nDNA dataset) support substantially younger ages for most interordinal divergences compared to many previous studies. However, the new dates do not resolve whether the early radiation of crown birds was a primarily Cretaceous versus Paleogene event due to the extension of the 95% HPD intervals for many divergences across the K-Pg boundary (tree file available at Dryad, <doi:10.5061/dryad.3c3r3>). One intractable issue in Bayesian divergence dating methods is that, due to the confounding effect of rate and time, posterior estimates of divergence time would retain some uncertainty even if an infinite amount of sequence data were available (dos Reis & Yang, 2013). Thus, currently favored divergence dating methods may lack the ability to distinguish a rapid Early Paleocene radiation from a Late Cretaceous radiation unless unreasonable strict priors are enforced, which would essentially answer the question before the analysis was initiated. Despite these limitations, it is worthwhile to test alternate scenarios in other ways. One simple test of the Paleogene radiation scenario is to assess whether implausible rates of evolution are required by a given set of assumptions. In the case of placental mammals, a recently articulated scenario of the explosive Early Paleocene radiation (O'Leary et al., 2013) was challenged on the basis that a large number of interordinal divergences occurring within 200 thousand years (Ka) of the Paleocene would require "virus-like" substitution rates (ca. 0.2 substitutions per nucleotide per million years) (Springer et al., 2013: 613). In the case of crown birds, it is possible to show that an explosive model does not require unreasonable assumptions regarding rates of sequence evolution. When priors are enforced so that all divergences except the Palaeognathae–Neognathae, Galloanserae–Neoaves, and Galliformes–Anseriformes splits are constrained to occur after the K-Pg

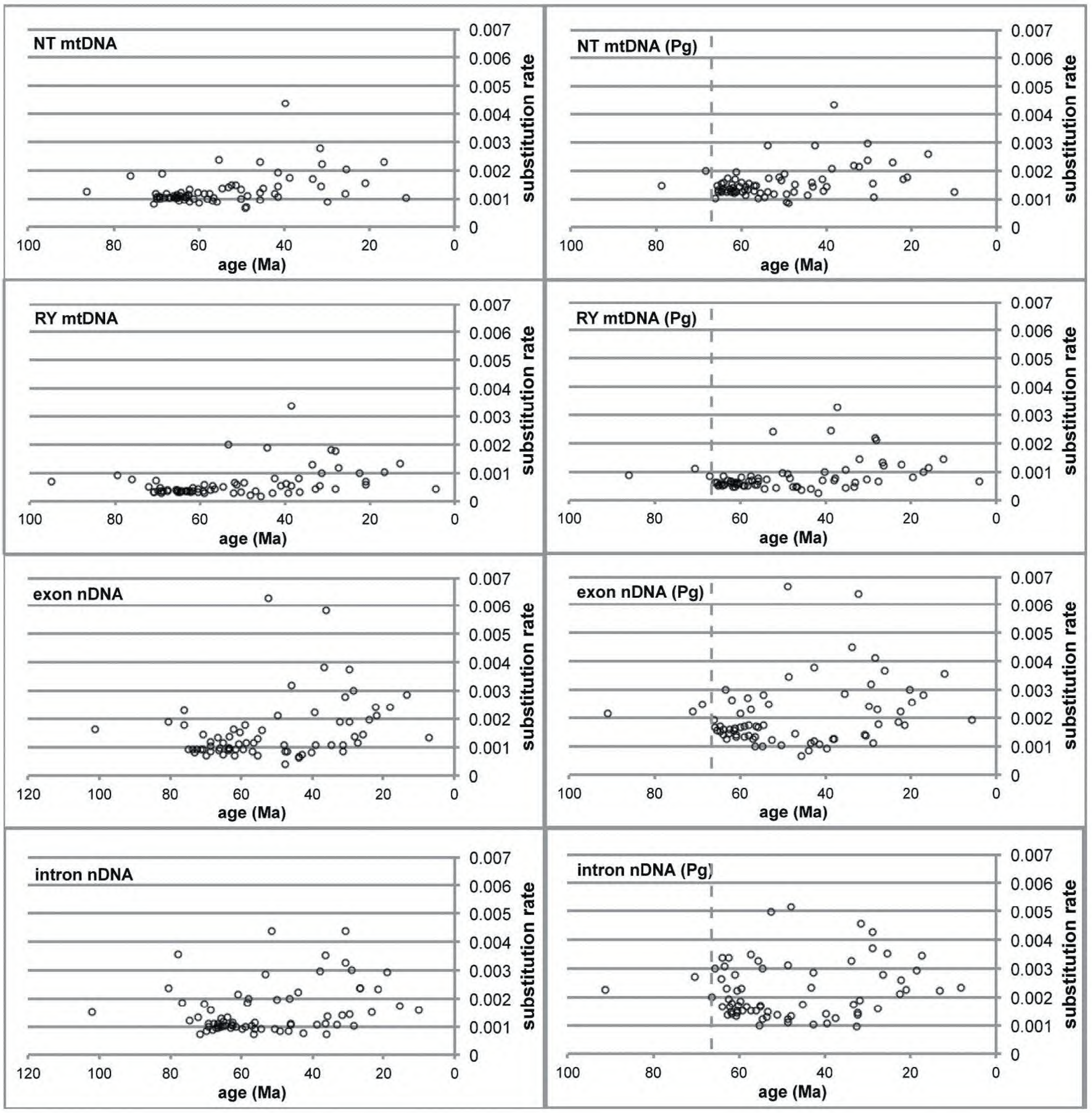


Figure 8. Inferred substitution rates (substitutions per site per million years) along branches leading to each dated node from fully calibrated analyses. Right-side graphs are from analyses in which additional maximum constraints were applied so that all divergences except those for the Palaeognathae, Neognathae, and Galloanserae are constrained to occur after the K-Pg boundary (66 Ma), as indicated by "Pg" notation.

boundary, no major substitution rate increase is observed for Paleocene divergences (Fig. 8). Indeed, the average Paleocene substitution rate is actually inferred to be lower than the average post-Paleocene substitution rate.

Beyond substitution rates, ecological factors deserve careful consideration. The number of lineages passing through the K-Pg boundary is an important indicator of the severity of the Cretaceous mass extinction of birds. Many molecular studies support dozens of major lineages that cross the K-Pg boundary, which at face value would represent an impressive survival rate during a mass extinction event. However, this represents only the tip of the iceberg, as previously noted in the case of placental mammals (Phillips, in press). Most avian divergence studies do not sample taxa completely, even at the ordinal level, and so may underestimate the lineages that would otherwise be placed in the Cretaceous in their results. Beyond this, even complete molecular sampling will detect only lineages leading to extant species, whereas birth–death models would predict the presence of some proportion of dead branches leading to now-extinct clades at any given point in time. Taking such factors into account, many molecular estimates of diversity across the Creta-

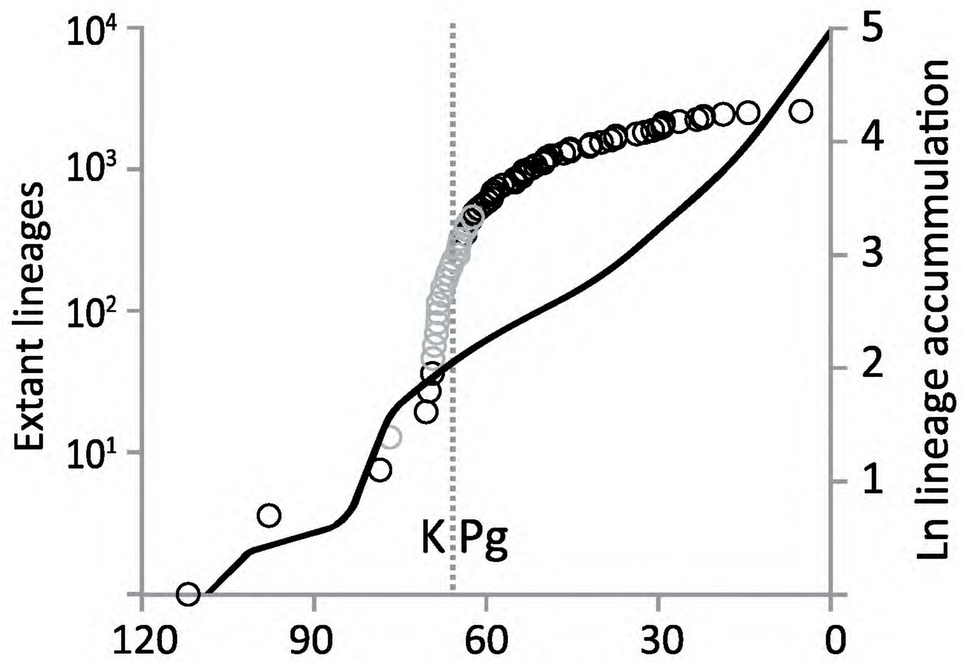


Figure 9. Lineage-through-time accumulations for Aves. Open circles represent ages inferred from the favored RY-mtDNA + exon nDNA fully calibrated relaxed clock analysis and are matched to the right scale. Gray circles indicate divergences that have 95% highest posterior density intervals that cross the K-Pg boundary. The solid line represents the lineage-through-time plot of Jetz et al. (2012) and is matched to the left scale.

ceous–Paleogene boundary are difficult to reconcile with the severity of this mass K-Pg extinction, which completely wiped out non-avian dinosaurs, pterosaurs, and previously successful archaic bird clades such as the Enantiornithes and Hesperornithes.

A related problem arises when one considers inferred diversification patterns during the Paleocene. Lineage-through-time analyses from studies supporting a major intraordinal diversification in the Cretaceous also suggest a significant diversification rate slowdown throughout the Paleocene (e.g., Jetz et al., 2012). Yet, it seems counterintuitive to posit a major slowdown in diversification rate during a time when crown birds should have been free to radiate into vacant ecological space opened up by the extinction of pterosaurs, all remaining stem bird lineages, and presumably many crown bird species. At the same time that a diversification slowdown should be occurring according to Jetz et al.'s (2012) lineage-through-time data, the fossil record records the rapid first appearances of many major lineages of birds and also supports a higher level of ecological diversity than seen in Cretaceous avifaunas (Mitchell & Makovicky, 2014). In contrast, our combined RY-coded mtDNA and exon nDNA analysis places the same explosive diversification of avian diversity near the K-Pg boundary, sufficiently close for the difference to potentially be explained by minor errors associated with tree extension and life history rate-correlations (Fig. 9).

Molecular phylogenetic analyses generally agree on the presence of a cluster of short internal branches near the base of Neoaves (e.g., Hackett et al., 2008; Pacheco et al., 2011). This cluster of short branches at the base of Neoaves (Fig. 2, node 17) is more easily reconciled with the fossil record and major events in Earth history by positing a rapid diversification in the aftermath of the Cretaceous–Paleogene extinction than a Cretaceous diversification followed by mass survival across the K-Pg boundary. Therefore, we lean toward interpreting the majority of divergences with HPD intervals overlapping the K-Pg boundary as Early Paleocene events. Given the difficulty in resolving temporal patterns in the early crown radiation of birds with molecular data only, focusing on the latest Cretaceous fossils will remain critical. Our preferred dates suggest that several lineages that represent the stems leading to multi-order clades may pass through the K-Pg boundary, and identifying fossil taxa that belong to these stem lineages will likely require both more complete specimens and more detailed morphological phylogenetic work.

Literature Cited

Alvarenga, H. M. F. 1983. Uma ave ratitae do Paleoceno Brasileiro: Bacia calcária de Itaboraí, Estado do Rio de Janeiro, Brasil. Bol. Mus. Nac., N. S., Geol. 41: 1–7.

Archibald, J. D. & D. H. Deutschman. 2001. Quantitative analysis of the timing of the origin and diversification of extant placental orders. J. Mammalian Evol. 8: 107–124.

Baker, A. J., S. L. Pereira & T. A. Paton. 2007. Phylogenetic relationships and divergence times of Charadriiformes genera: Multigene evidence for the Cretaceous origin of at least 14 clades of shorebirds. Biol. Lett. 3: 205–209.

Barker, F. K., A. Cibois, P. Schikler, J. Feinstein & J. Cracraft. 2004. Phylogeny and diversification of the largest avian radiation. Proc. Natl. Acad. Sci. U.S.A. 101: 11040–11045.

Benton, M. J. & P. C. J. Donoghue. 2007. Paleontological evidence to date the tree of life. Molec. Biol. Evol. 24: 26–53.

Benton, M. J., P. C. J. Donoghue & R. J. Asher. 2009. Calibrating and constraining molecular clocks. Pp. 35–86 *in* S. B. Hedges & S. Kumar (editors), The TimeTree of Life. Oxford University Press, Oxford.

Bertelli, S. & L. M. Chiappe. 2005. Earliest tinamous (Aves: Palaeognathae) from the Miocene of Argentina and their phylogenetic position. Contr. Sci. Nat. Hist. Mus. Los Angeles County 502: 1–20.

Bininda-Emonds, O. R. P., M. Cardillo, K. E. Jones, R. D. E. MacPhee, M. R. D. Beck, R. Grenyer, S. A. Price, R. A. Vos, J. L. Gittleman & A. Purvis. 2007. The delayed rise of placental mammals. Nature 446: 507–512.

Boles, W. E. 1995. The world's oldest songbird. Nature 374: 21–22.

Boles, W. E. 1997. Fossil songbirds (Passeriformes) from the early Eocene of Australia. Emu 97: 43–50.

Bourdon, E., B. Bouya & M. Iarochene. 2005. Earliest African neornithine bird: A new species of Prophaethontidae (Aves) from the Paleocene of Morocco. J. Vertebrate Paleontol. 25: 157–170.

Bourdon, E., C. Mourer-Chauviré, M. Amaghzaz & B. Bouya. 2008. New specimens of *Lithoptila abdounensis* (Aves, Prophaethontidae) from the Lower Paleogene of Morocco. J. Vertebrate Paleontol. 28: 751–761.

Bromham, L. 2011. The genome as a life-history character: Why rate of molecular evolution varies between mammal species. Philos. Trans., Ser. B 366: 2503–2513.

Brown, J. W. & M. van Tuinen. 2011. Evolving perceptions on the antiquity of the modern avian tree. Pp. 306–324 *in* G. Dyke & G. Kaiser (editors), Living Dinosaurs: The Evolutionary History of Modern Birds. Wiley-Blackwell, Chichester.

Brown, J. W., R. B. Payne & D. P. Mindell. 2007. Nuclear DNA does not reconcile 'rocks' and 'clocks' in Neoaves: A comment on Ericson et al. Biol. Lett. 3: 257–260.

Brown, J. W., J. Rest, J. Garcia-Moreno, M. Sorenson & D. Mindell. 2008. Strong mitochondrial DNA support for a Cretaceous origin of modern avian lineages. BMC Biol. 6: 6.

Cande, S. C. & J. M. Stock. 2004. Cenozoic Reconstructions of the Australia-New Zealand-South Pacific Sector of Antarctica. The Cenozoic Southern Ocean: Tectonics, Sedimentation, and Climate Change between Australia and Antarctica. Amer. Geophys. Union, Geophys. Monogr. Ser. 151: 5–17.

Cavender, J. A. & J. Felsenstein. 1987. Invariants of phylogenies in a simple case with discrete states. J. Classific. 4: 57–71.

Chambers, L. M., M. Pringle, G. Fitton, L. M. Larsen, A. K. Pedersen & R. Parrish. 2003. Recalibration of the Palaeocene-Eocene boundary (P-E) using high precision U-Pb and Ar-Ar isotopic dating. Pp. 9681–9682 *in* Geophysical Research Abstracts, EGS-AGU-EUG Joint Assembly, Nice, France, 6–11 April 2003.

Clarke, J. A. 2004. Morphology, phylogenetic taxonomy, and systematics of *Ichthyornis* and *Apatornis* (Avialae: Ornithurae). Bull. Amer. Mus. Nat. Hist. 286: 1–179.

Clarke, J. A. & M. A. Norell. 2004. New avialan remains and a review of the known avifauna from the Late Cretaceous Nemegt Formation of Mongolia. Amer. Mus. Novit. No. 3447: 1–2.

Clarke, J. A., C. P. Tambussi, J. I. Noriego, G. M. Erickson & R. A. Ketcham. 2005. Definitive fossil evidence for the extant avian radiation in the Cretaceous. Nature 433: 305–308.

Clarke, J. A., D. T. Ksepka, N. A. Smith & M. A. Norell. 2009. Combined phylogenetic analysis of a new North American fossil species confirms widespread Eocene distribution for stem rollers (Aves, Coracii). Zool. J. Linn. Soc. 157: 586–611.

Cooper, A. & D. Penny. 1997. Mass survival of birds across the Cretaceous–Tertiary boundary: Molecular evidence. Science 275: 1109–1113.

Cooper, A., C. Lalueza-Fox, S. Anderson, A. Rambaut, J. Austin & R. Ward. 2001. Complete mitochondrial genome sequences of two extinct moas clarify ratite evolution. Nature 409: 704–707.

Cooper, R. A. 2004. The New Zealand Geological Timescale. Institute of Geological and Nuclear Sciences, Lower Hutt, New Zealand.

Cracraft, J. 2001. Avian evolution, Gondwana biogeography and the Cretaceous–Tertiary mass extinction event. Proc. Roy. Soc. London, Ser. B, Biol. Sci. 268: 459–469.

dos Reis, M. & Z. Yang. 2013. The unbearable uncertainty of Bayesian divergence time estimation. J. Syst. Evol. 51: 30–43.

dos Reis, M., J. Inoue, M. Hasegawa, R. J. Asher, P. C. J. Donoghue & Z. Yang. 2012. Phylogenomic datasets provide both precision and accuracy in estimating the timescale of placental mammal phylogeny. Proc. Roy. Soc. London, Ser. B, Biol. Sci. 279: 3491–3500.

Drummond, A. J. & A. Rambaut. 2007. BEAST: Bayesian evolutionary analysis by sampling trees. BMC Biol. 7: 214.

Drummond, A. J., S. Y. W. Ho, M. J. Phillips & A. Rambaut. 2006. Relaxed phylogenetics and dating with confidence. PLoS Biol. 4: 699.

Dunning, Jr., J. B. 2007. CRC Handbook of Avian Body Masses, 2nd ed. CRC Press, Boca Raton.

Dyke, G. J. & J. H. Cooper. 2000. A new psittaciform bird from the London Clay (Lower Eocene) of England. Palaeontology 43: 271–285.

Edgar, R. C. 2004a. MUSCLE: Multiple sequence alignment with high accuracy and high throughput. Nucleic Acids Res. 32: 1792–1797.

Edgar, R. C. 2004b. MUSCLE: A multiple sequence alignment method with reduced time and space complexity. BMC Bioinf. 5: 113.

Ericson, P. G. P., L. Christidis, A. Cooper, M. Irestedt, J. Jackson, U. S. Johannson & J. A. Norman. 2002. A Gondwanan origin of passerine birds supported by DNA sequences of the endemic New Zealand wrens. Proc. Roy. Soc. London, Ser. B, Biol. Sci. 269: 235–241.

Ericson, P. G. P., C. L. Anderson, T. Britton, A. Elzanowski, U. S. Johansson, M. Källersjö, J. I. Ohlson, T. J. Parsons, D. Zuccon & G. Mayr. 2006. Diversification of Neoaves: Integration of molecular sequence data and fossils. Biol. Lett. 4: 543–547.

Ericson, P. G. P., C. L. Anderson & G. Mayr. 2007. Hangin' on to our rocks 'n clocks: A reply to Brown et al. Biol. Lett. 3: 260.

Feduccia, A. 1995. Explosive evolution in Tertiary birds and mammals. Science 267: 637–638.

Franzen, J. F. 2005. The implications of the numerical dating of the Messel fossil deposit (Eocene, Germany) for mammalian biochronology. Ann. Paleontol. 91: 329–335.

Gradstein, F. M., J. G. Ogg, M. Schmitz & G. Ogg. 2012. Geological Time Scale 2012. Elsevier Science and Technology, Amsterdam.

Hackett, S. J., R. T. Kimball, S. Reddy, R. C. K. Bowie, E. L. Braun, M. J. Braun, J. L. Chojnowski, W. A. Cox, K.-L. Han, J. Harshman, C. J. Huddleston, B. D. Marks, K. J. Miglia, W. S. Moore, F. H. Sheldon, D. W. Steadman, C. C. Witt & T. Yuri. 2008. A phylogenomic study of birds reveals their evolutionary history. Science 320: 1763–1768.

Haddrath, O. & A. J. Baker. 2012. Multiple nuclear genes and retroposons support vicariance and dispersal of the palaeognaths, and an Early Cretaceous origin of modern birds. Proc. Roy. Soc. London, Ser. B, Biol. Sci. 279: 4617–4625.

Harrison, G. L., P. A. McLenachan, M. J. Phillips, K. E. Slack, A. Cooper & D. Penny. 2004. Four new avian mitochondrial genomes help get to basic evolutionary questions in the Late Cretaceous. Molec. Biol. Evol. 21: 974–983.

Hendy, M. D. & D. Penny. 1989. A framework for the quantitative study of evolutionary trees. Syst. Zool. 38: 297–309.

Houde, P. W. 1988. Paleognathous Birds from the Early Tertiary of the Northern Hemisphere. Nuttall Ornithological Club, Cambridge.

Hugall, A. F., R. Foster & M. S. Y. Lee. 2007. Calibration choice, rate smoothing, and the pattern of tetrapod diversification according to the long nuclear gene RAG-1. Syst. Biol. 56: 543–563.

Jarvis, E. D., S. Mirarab, A. J. Aberer, et al. 2014. Whole-genome analyses resolve early branches in the tree of life of modern birds. Science 346: 1320–1331.

Jetz, W., G. H. Thomas, J. B. Joy, K. Hartmann & A. O. Mooers. 2012. The global diversity of birds in space and time. Nature 491: 444–448.

Kitazoe, Y., H. Kishino, P. J. Waddell, N. Nakajima, T. Okabayashi, T. Watanabe & Y. Okuhara. 2007. Robust time estimation reconciles views of the antiquity of placental mammals. PLoS ONE 2: e384.

Kolaczkowski, B. & J. W. Thornton. 2004. Performance of maximum parsimony and likelihood phylogenetics when evolution is heterogeneous. Nature 431: 980–984.

Kristoffersen, A. V. 2002. An early Paleogene trogon (Aves: Trogoniformes) from the Fur Formation, Denmark. J. Vertebrate Paleontol. 22: 661–666.

Ksepka, D. T. 2009. Broken gears in the avian molecular clock: New phylogenetic analyses support stem galliform status for *Gallinuloides wyomingensis* and rallid affinities for *Amitabha urbsinterdictensis*. Cladistics 25: 173–197.

Ksepka, D. T. & J. A. Clarke. 2015. Phylogenetically vetted and stratigraphically constrained fossil calibrations within Aves. Palaeontol. Electronica 18.1.3FC: 1–25.

Ksepka, D. T., S. Bertelli & N. P. Giannini. 2006. The phylogeny of the living and fossil Sphenisciformes (penguins). Cladistics 22: 412–441.

Ksepka, D. T., J. A. Clarke & L. Grande. 2011. Stem parrots (Aves, Halcyornithidae) from the Green River Formation and a combined phylogeny of Pan-Psittaciformes. J. Paleontol. 85: 835–854.

Ksepka, D. T., J. A. Clarke, S. J. Nesbitt, F. Kulpe & L. Grande. 2013. Fossil evidence of wing shape in a stem relative of swifts and hummingbirds (Aves, Pan-Apodiformes). Proc. Roy. Soc. London, Ser. B, Biol. Sci. 280: 20130580.

Ksepka, D. T., J. L. Ware & K. S. Lamm. 2014. Flying rocks and flying clocks: Disparity in fossil and molecular dates for birds. Proc. Roy. Soc. London, Ser. B, Biol. Sci. 281: 20140677.

Lanfear, R., B. Calcott, S. Y. W. Ho & S. Guindon. 2012. PartitionFinder: Combined selection of partitioning schemes and substitution models for phylogenetic analyses. Molec. Biol. Evol. 29: 1695–1701.

Lartillot, N. & F. Delsuc. 2012. Joint reconstruction of divergence times and life-history evolution in placental mammals using a phylogenetic covariance model. Evolution 66: 1773–1787.

Longrich, N. R., T. Tokaryk & D. J. Field. 2011. Mass extinction of birds at the Cretaceous–Paleogene (K–Pg) boundary. Proc. Natl. Acad. Sci. U.S.A. 108: 15253–15257.

Louchart, A., N. Tourment & J. Carrier. 2011. The earliest known pelican reveals 30 million years of evolutionary stasis in beak morphology. J. Ornithol. 152: 15–20.

Manegold, A. 2008. Passerine diversity in the late Oligocene of Germany: Earliest evidence for the sympatric coexistence of Suboscines and Oscines. Ibis 150: 377–387.

Mayr, G. 2003. Phylogeny of early Tertiary swifts and hummingbirds (Aves: Apodiformes). Auk 120: 145–151.

Mayr, G. 2004. A partial skeleton of a new fossil loon (Aves, Gaviiformes) from the early Oligocene of Germany with preserved stomach content. J. Ornithol. 145: 281–286.

Mayr, G. 2005a. The Paleogene fossil record of birds in Europe. Biol. Rev. 80: 515–542.

Mayr, G. 2005b. The postcranial osteology and phylogenetic position of the Middle Eocene *Messelastur gratulator* Peters, 1994: A morphological link between owls (Strigiformes) and falconiform birds? J. Vertebrate Paleontol. 25: 635–645.

Mayr, G. 2005c. A new cypselomorph bird from the middle Eocene of Germany and the early diversification of avian aerial insectivores. Condor 107: 342–352.

Mayr, G. 2007. A small representative of the Phalacrocoracoidea (cormorants and anhingas) from the Late Oligocene of Germany. Condor 109: 929–942.

Mayr, G. 2009. Paleogene Fossil Birds. Springer, Heidelberg.

Mayr, G. 2013. The age of the crown group of passerine birds and its evolutionary significance—Molecular calibrations versus the fossil record. Syst. & Biodivers. 11: 7–13.

Mayr, G. 2014a. The origins of crown group birds: Molecules and fossils. Palaeontology 57: 231–242.

Mayr, G. 2014b. A new skeleton of the late Oligocene "Enspel cormorant"—From *Oligocorax* to *Borvocarbo*, and back again. Palaeobiodivers. & Palaeoenvironm. 95: 87–101.

Mayr, G. 2015. Skeletal morphology of the middle Eocene swift *Scaniacypselus* and the evolutionary history of true swifts (Apodidae). J. Ornithol. 156: 411–450.

Mayr, G. & S. Bertelli. 2011. A record of *Rhynchaeites* (Aves, Threskiornithidae) from the early Eocene Fur Formation of Denmark, and the affinities of the alleged parrot *Mopsitta*. Palaeobiodivers. & Palaeoenvironm. 91: 229–236.

Mayr, G., C. Mourer-Chauviré & I. Weidig. 2004. Osteology and systematic position of the Eocene Primobucconidae (Aves, Coraciiformes *sensu stricto*), with first records from Europe. J. Syst. Palaeontol. 2: 1–12.

Mayr, G., M. Porschmann & M. Wuttke. 2006. A nearly complete skeleton of the fossil galliform bird *Palaeortyx* from the late Oligocene of Germany. Acta Ornithol. 41: 129–135.

Meredith, R. W., J. E. Janecka, J. Gatesy, O. A. Ryder, C. A. Fisher, E. C. Teeling, A. Goodbla, E. Eizirik, T. T. L. Simão, T. Stadler, D. L. Rabosky, R. L. Honeycutt, J. J. Flynn, C. M. Ingram, C. Steiner, T. L. Williams, T. J. Robinson, A. Burk-Herrick, M. Westerman, N. A. Ayoub, M. S. Springer & W. J. Murphy. 2011. Impacts of the Cretaceous terrestrial revolution and the KPg extinction on mammal diversification. Science 334: 521–524.

Mertz, D. F., F.-J. Harms, G. Gabriel, & M. Felder. 2004. Arbeitstreffen in der Forschungsstation Grube Messel mit neuen Ergebnissen aus der Messel-Forschun. Natur & Mus. 134: 289–290.

Mertz, L. F., P. R. Renne, M. Wuttke & C. Mödden. 2007. A numerically calibrated reference level (MP28) for the terrestrial mammal based biozonation of the European Upper Oligocene. Int. J. Earth Sci. 96: 353–361.

Mitchell, J. S. & P. J. Makovicky. 2014. Low ecological disparity in Early Cretaceous birds. Proc. Roy. Soc. London, Ser. B, Biol. Sci. 281: 20140608.

Morgan, C. C., C. J. Creevey & M. J. O'Connell. 2014. Mitochondrial data are not suitable for resolving placental mammal phylogeny. Mammalian Genome 25: 636–647.

Morgan-Richards, M., S. A. Trewick, A. Bartosch-Härlid, O. Kardailsky, M. J. Phillips, P. A. McLenanchan & D. Penny. 2008. Bird evolution: Testing the Metaves clade with six new mitochondrial genomes. BMC Evol. Biol. 8: 20.

Nabholz, B., S. Glémin & N. Galtier. 2008. Strong variations of mitochondrial mutation rate across mammals: The longevity hypothesis. Molec. Biol. Evol. 25: 120–130.

Ogg, J. G., G. Ogg & F. M. Gradstein. 2008. The Concise Geologic Time Scale. Cambridge University Press, Cambridge.

O'Leary, M. A., J. I. Bloch, J. J. Flynn, T. J. Gaudin, A. Giallombardo, N. P. Giannini, S. L. Goldberg, B. P. Kraatz, Z.-X. Luo, J. Meng, X. Ni, M. J. Novacek, F. A. Perini, Z. S. Randall, G. W. Rougier, E. J. Sargis, M. T. Silcox, N. B. Simmons, M. Spaulding, P. M. Velazco, M. Weksler, J. R. Wible & A. L. Cirranello. 2013. The placental mammal ancestor and the post–K-Pg radiation of placentals. Science 339: 662–667.

Olson, S. L. 1977. A Lower Eocene frigatebird from the Green River Formation of Wyoming (Pelecaniformes, Fregatidae). Smithsonian Contr. Paleontol. 35: 1–33.

Olson, S. L. 1985. The fossil record of birds. Pp. 79–238 *in* D. S. Farner, J. R. King & K. C. Parkes (editors), Avian Biology. Academic Press, New York.

Pacheco, M. A., F. U. Battistuzzi, M. Lentino, R. F. Aguilar, S. Kumar & A. A. Escalante. 2011. Evolution of modern birds revealed by mitogenomics: Timing the radiation and origin of major orders. Molec. Biol. Evol. 28: 1927–1942.

Parham, J. F., P. C. J. Donoghue, C. J. Bell, T. D. Calway, J. J. Head, P. A. Holroyd, J. G. Inoue, R. B. Irmis, W. G. Joyce, D. T. Ksepka, J. S. L. Patané, N. D. Smith, J. E. Tarver, M. van Tuinen, Z. Yang, K. D. Angielczyk, J. Greenwood, C. A. Hipsley, L. Jacobs, P. J. Makovicky, J. Müller, K. T. Smith, J. M. Theodor, R. C. M. Warnock & M. J. Benton. 2012. Best practices for justifying fossil calibrations. Syst. Biol. 61: 346–359.

Perkins, M. E., J. G. Fleagle, M. T. Heizler, B. Nash, T. M. Bown, A. Tauber & M. T. Dozo. 2012. Tephrochronology of the Miocene Santa Cruz and Pinturas Formations, Argentina. Pp. 23–40 *in* S. F. Vizcaíno, R. F. Kay & M. Susana Bargo (editors), Early Miocene Paleobiology in Patagonia: High-Latitude Paleocommunities of the Santa Cruz Formation. Cambridge University Press, Cambridge.

Phillips, M. J. 2009. Branch-length estimation bias misleads molecular dating for a vertebrate mitochondrial phylogeny. Gene 441: 132–140.

Phillips, M. J. 2015. Four mammal fossil calibrations: Balancing competing palaeontological and molecular considerations. Palaeontol. Electronica 18.1.5FC: 1–16.

Phillips, M. J. & D. Penny. 2003. The root of the mammalian tree inferred from whole mitochondrial genomes. Molec. Phylogen. Evol. 28: 171–185.

Phillips, M. J., T. H. Bennett & M. S. Y. Lee. 2009. Molecules, morphology and ecology indicate a recent, amphibious origin for echidnas. Proc. Natl. Acad. Sci. U.S.A. 106: 17089–17094.

Phillips, M. J., G. C. Gibb, E. A. Crimp & D. Penny. 2010. Tinamous and moa flock together: Mitochondrial genome sequence analysis reveals independent losses of flight among ratites. Syst. Biol. 59: 90–107.

Posada, D. 2008. jModelTest: Phylogenetic model averaging. Molec. Biol. Evol. 25: 1253–1256.

Rambaut, A. 1996. Sequence alignment editor. Available at <http://tree.bio.ed.ac.uk/software/seal>, accessed 30 April 2015.

Rambaut, A. & N. C. Grassly. 1997. Seq-Gen: An application for Monte Carlo simulation of DNA sequence evolution along phylogenetic trees. Computer Applic. Biosci. 13: 235–238.

Rambaut, A. & A. J. Drummond. 2007. Tracer version 1.4. Computer program and documentation distributed by the author. <http://beast.bio.ed.ac.uk/Tracer>, accessed 6 February 2015.

Raup, D. M. 1972. Taxonomic diversity during the Phanerozoic. Science 177: 1065–1071.

Sansom, R. S. & M. A. Wills. 2013. Fossilization causes organisms to appear erroneously primitive by distorting evolutionary trees. Sci. Rep. 3: 2545.

Sansom, R. S., S. Gabbott & M. A. Purnell. 2010. Non-random decay of chordate characters causes bias in fossil interpretation. Nature 463: 797–800.

Sansom, R. S., S. Gabbott & M. A. Purnell. 2011. Decay of vertebrate characters in hagfish and lamprey (Cyclostomata) and the implications for the vertebrate fossil record. Proc. Roy. Soc. London, Ser. B, Biol. Sci. 1709: 1150–1157.

Siddall, M. 1998. Success of parsimony in the four-taxon case: Long-branch repulsion by likelihood in the Farris zone. Cladistics 14: 209–220.

Simpson, G. G. 1945. The principles of classification and a classification of mammals. Bull. Amer. Mus. Nat. Hist. 85: 1–350.

Slack, K. E., C. M. Jones, T. Ando, G. L. Harrison, R. E. Fordyce, U. Arnason & D. Penny. 2006. Early penguin fossils, plus mitochondrial genomes, calibrate avian evolution. Molec. Biol. Evol. 23: 1144–1155.

Smith, M. E., A. R. Carroll & B. S. Singer. 2008. Synoptic reconstruction of a major ancient lake system: Eocene Green River Formation, western United States. GSA Bull. 120: 54–84.

Smith, N. A. 2015. Sixteen vetted fossil calibrations for divergence dating of Charadriiformes (Aves, Neognathae). Palaeontol. Electronica 18.1.4FC: 1–18.

Smith, N. D. 2010. Phylogenetic analysis of Pelecaniformes (Aves) based on osteological data: Implications for waterbird phylogeny and fossil calibration studies. PLoS ONE 5: e13354.

Smith, N. D. & D. T. Ksepka. 2015. Five well-supported fossil calibrations within the "Waterbird" assemblage (Tetrapoda, Aves). Palaeontol. Electronica 18.1.7FC: 1–20.

Springer, M. S., R. W. DeBry, C. J. Douady, H. M. Amrine, O. Madsen, W. W. de Jong & M. J. Stanhope. 2001. Mitochondrial versus nuclear gene sequences in deep-level phylogeny reconstruction. Molec. Biol. Evol. 18: 132–143.

Springer, M. S., W. J. Murphy, E. Eizirik & S. J. O'Brien. 2003. Placental mammal diversification and the Cretaceous–Tertiary boundary. Proc. Natl. Acad. Sci. U.S.A. 100: 1056–1061.

Springer, M. S., M. Scally, O. Madsen, W. W. De Jong, C. J. Douady & M. J. Stanhope. 2004. The use of composite taxa in supermatrices. Molec. Phylogen. Evol. 30: 883–884.

Springer, M. S., R. W. Meredith, E. C. Teeling & W. J. Murphy. 2013. Comment on "The placental mammal ancestor and the post–K-Pg radiation of placentals." Science 341: 613.

Storch, G., B. Engesser & M. Wuttke. 1996. Oldest fossil record of gliding in rodents. Nature 379: 439–441.

Swofford, D. L. 2002. PAUP*: Phylogenetic Analysis Using Parsimony (* and Other Methods), Version 4.0b10. Sinauer Associates, Inc., Sunderland, Massachusetts.

Szyndlar, Z. 1994. Oligocene snakes of southern Germany. J. Vertebrate Paleontol. 14: 24–37.

Trewick, S. A. & G. C. Gibb. 2010. Vicars, tramps and assembly of the New Zealand avifauna: A review of molecular phylogenetic evidence. Ibis 152: 226–253.

van Tuinen, M. & E. A. Hadly. 2004. Error in estimation of rate and time inferred from the early amniote fossil record and avian molecular clocks. J. Molec. Evol. 59: 267–276.

Waddell, P. J., H. Kishino & R. Ota. 2001. A phylogenetic foundation for comparative mammalian genomics. Genome Informatics 12: 141–154.

Welch, J. J., O. R. Bininda-Emonds & L. B. Bromham. 2008. Correlates of substitution rate variation in mammalian protein-coding sequences. BMC Evol. Biol. 8: 53.

Westerhold, T., U. Röhl, J. Laskar, I. Raffi, J. Bowles, L. J. Lourens & J. C. Zachos. 2007. On the duration of magnetochrons C24r and C25n and the timing of early Eocene global warming events: Implications from the Ocean Drilling Program Leg 208 Walvis Ridge depth transect. Paleoceanography 22: PA2201.

Wible, J. R., G. W. Rougier, M. J. Novacek & R. J. Asher. 2007. Cretaceous eutherians and Laurasian origin for placental mammals near the K/T boundary. Nature 447: 1003–1006.

Wijnker, E. & S. L. Olson. 2009. A revision of the fossil genus *Miocepphus* and other Miocene Alcidae (Aves: Charadriiformes) of the western North Atlantic Ocean. J. Syst. Palaeontol. 7: 471–487.

Wolfe, K. H., W.-H. Li & P. M. Sharp. 1987. Rates of nucleotide substitution vary greatly among plant mitochondrial, chloroplast and nuclear DNAs. Proc. Natl. Acad. Sci. U.S.A. 84: 9054–9058.

Woodburne, M. O., B. J. MacFadden, J. A. Case, M. S. Springer, N. S. Pledge, J. D. Power, J. M. Woodburne & K. B. Springer. 1994. Land mammal biostratigraphy and magnetostratigraphy of the Etadunna Formation (Late Oligocene) of South Australia. J. Vertebrate Paleontol. 13: 483–515.

Worthy, T. H., J. P. Worthy, A. J. D. Tennyson, S. W. Salisbury, S. J. Hand & R. P. Scofield. 2013. Miocene fossils show that kiwi (*Apteryx*, Apterygidae) are probably not phyletic dwarves. Pp. 63–80 *in* U. B. Göhlich & A. Kroh (editors), Paleornithological Research 2013. Proceedings of the 8th International Meeting Society of Avian Paleontology and Evolution. Naturhistorisches Museum, Vienna.

Worthy, T. H., S. J. Hand & M. Archer. 2014. Phylogenetic relationships of the Australian Oligo–Miocene ratite *Emuarius gidju* Casuariidae. Integr. Zool. 9: 148–166.

Wright, T. F., E. E. Schirtzinger, T. Matsumoto, J. R. Eberhard, G. R. Graves, J. J. Sanchez, S. Capelli, H. Muller, J. Scharpegge, G. K. Chambers & R. C. Fleischer. 2008. A multilocus molecular phylogeny of the parrots (Psittaciformes): Support for a Gondwanan origin during the Cretaceous. Molec. Biol. Evol. 25: 2141–2156.

Yang, Z. & B. Rannala. 2006. Bayesian estimation of species divergence times under a molecular clock using multiple fossil calibrations with soft bounds. Molec. Biol. Evol. 23: 212–226.

Appendix 1. Fossil calibrations used in this study.

Node Calibrated: Casuariiformes (*Dromaius* + *Casuarius*)

Fig. 2, node 6.

Prior shape. Uniform.

Fossil specimen. †*Emuarius gidju* (QM F45460).

Phylogenetic justification. Worthy et al. (2014) recovered †*Emuarius* as more closely related to *Dromaius* than *Casuarius* in a phylogenetic analysis. Codings for †*Emuarius* were based on multiple specimens, and key synapomorphies occur in the skull, tarsometatarsus, and scapulocoracoid. We have thus selected a scapulocoracoid (QM F45460) as the calibrating specimen, although it should be noted that other elements also occur at the same site.

Hard minimum age. 24.5 Ma.

Minimum age justification. QM F45460 was collected from Faunal Zone A at the Hiatus South Site of the Riversleigh locality in Queensland, Australia. Based on biocorrelation to the faunas from the Etadunna and Namba Formations in South Australia (Woodburne et al., 1994), a minimum age matching the top of Chron 7r is applied, with the numerical date selected from table 28.2 of Gradstein et al. (2012).

Soft maximum age. 58.7 Ma.

Maximum age justification. The soft maximum is based on the age of the oldest putative Palaeognathae, which include Middle–Late Paleocene lithornithids from North America (Houde, 1988) and the ratite †*Diogenornis*, from the Early Eocene of Brazil (Alvarenga, 1983). While the precise phylogenetic relationships of these taxa are debated, none are plausibly nested within crown Casuariiformes.

Node Calibrated: Tinamiformes (Nothurinae + Tinaminae)

Fig. 2, node 8.

Prior shape. Uniform.

Fossil specimen. Tinamidae sp. indet. (MACN-SC-1399).

Phylogenetic justification. A phylogenetic analysis by Bertelli and Chiappe (2005) placed MACN-SC-1399 within the crown clade Tinamidae, along the stem lineage leading to Nothurinae (aridland tinamous).

Hard minimum age. 16.9 Ma.

Minimum age justification. MACN-SC-1399 was collected from the Pinturas Formation of Argentina. The hard minimum age is based on a radiometric date from a tuff that lies on the boundary between Pinturas Formation and Santa Cruz Formation (Perkins et al., 2012).

Soft maximum age. 58.7 Ma.

Maximum age justification. The soft maximum is based on the age of the oldest putative Palaeognathae, which include Middle–Late Paleocene lithornithids from North America (Houde, 1988) and the ratite †*Diogenornis*, from the Early

Eocene of Brazil (Alvarenga, 1983). While the precise phylogenetic relationships of these taxa are debated, none are plausibly nested within the crown Tinamiformes.

Node Calibrated: Galliformes (Megapodidae + Numididae + Phasianidae)
Fig. 2, node 11.

Prior shape. Uniform.
Fossil specimen. †*Palaeortyx brevipes* (PW 2005/5023a-LS).
Phylogenetic justification. Mayr et al. (2006) described apomorphies, including the well-developed processus intermetacarpalis, that support placement of †*Palaeortyx brevipes* within crown Galliformes, as a stem representative of Phasianidae. PW 2005/5023a-LS represents a nearly complete skeleton and thus is selected as the calibrating specimen.
Hard minimum age. 24.0 Ma.
Minimum age justification. PW 2005/5023a-LS was collected from a maar lake deposit at Enspel, near Bad Marienberg in Westerwald, Rheinland-Pfalz, Germany. These deposits are assigned to the MP28 biozone (Storch et al., 1996), the top of which is used for the hard minimum age.
Soft maximum age. 51.57 Ma.
Maximum age justification. The soft maximum is based on the age of the Green River Formation from which multiple complete skeletons of the stem galliform †*Gallinuloides wyomingensis* have been collected. This maximum encompasses other strata that have yielded good material of stem galliforms but no convincing crown galliform material, including the Messel Formation, Eocene horizons at Quercy, and the London Clay Formation. Although the minimum age we specified is likely to be extended backward in time with future revisions of the galliform fossil record, the uniform prior accommodates this by encompassing the ages of taxa that may possibly represent crown galliforms but require additional study, such as †*Procrax* and †*Schaubortyx*.

Node Calibrated: Anatoidea (Anatidae + Anseranatidae)
Fig. 2, node 14.

Prior shape. Approximate lognormal.
Fossil specimen. †*Vegavis iaai* (MLP 93-I-3-1).
Phylogenetic justification. Phylogenetic analyses by Clarke et al. (2005) placed †*Vegavis* (which is known only from the holotype MLP 93-I-3-1) within Anseriformes, along the stem lineage leading to Anatidae.
Hard minimum age. 66 Ma.
Minimum age justification. MLP 93-I-3-1 was collected from near the lower base of the dinoflagellate *Manumiella bertodano* biozone in lithostratigraphic unit K3, also referred to as Unit "C," or the Sandwich Bluff Member, of the Lopez de Bertodano Formation at Sandwich Bluff, Vega Island, Antarctica. The minimum age is based on the age of the *M. bertodano* biozone as well as the inferred sedimentation rate.
Soft maximum age. 86.3 Ma.
Maximum age justification. The soft maximum is based on the lower bound of the Santonian stage. This accounts for the presence of numerous stem birds and absence of crown birds of any type, let alone Anseriformes, throughout this part of the Late Cretaceous (after Benton & Donoghue, 2007).

Node Calibrated: Unnamed Clade (Phaethontiformes + Columbiformes)
Fig. 2, node 21.

Prior shape. Approximate lognormal.
Fossil specimen. †*Lithoptila abdounensis* (OCP.DEK/GE 1087).
Phylogenetic justification. Phylogenetic analyses by Bourdon et al. (2005) and Smith (2010) recovered †*Lithoptila abdounensis* as a stem representative of Phaethontidae, and cranial characters preserved in OCP.DEK/GE 1087 support this placement. Although the position of Phaethontidae within Aves is controversial, there is no doubt regarding the placement of †*Lithoptila*, which tracks Phaethontidae regardless of the arrangement of other taxa. Therefore, the calibration is placed at the node uniting Phaethontiformes and Columbiformes in the present study.
Hard minimum age. 56.0 Ma.
Minimum age justification. OCP.DEK/GE 1087 was collected from an unspecified quarry, assigned to Bed IIa of the Ouled Abdoun Basin, near Grand Daoui, Morocco, which in turn can be assigned to the Thanetian based on selachians identified in the matrix (Bourdon et al., 2005). As both the precise numerical age of Bed IIa deposits and the precise horizon from which the *Lithoptila abdounensis* holotype was collected remain uncertain, the lower age bound for the Thanetian is used as a hard minimum.
Soft maximum age. 72.1 Ma.
Maximum age justification. The maximum age extends to the base of Maastrichtian to accommodate the possibility that some of the poorly represented marine birds from the Cretaceous–Paleogene of New Jersey, U.S.A., may represent tropicbirds (Bourdon et al., 2008).

Node Calibrated: Apodiformes (Apodidae + Trochilidae)
Fig. 2, node 25.

Prior shape. Uniform.
Fossil specimen. †*Scaniacypselus szarskii* (SMF-ME 11345A+B).
Phylogenetic justification. Phylogenetic analysis of morphological data (Mayr, 2003, 2005c) and combined morphological and molecular data (Ksepka et al., 2013) supports the placement of †*Scaniacypselus szarskii* as a stem member of Apodidae. Several characters of the wing are optimized as synapomorphies supporting this position, and can be observed in the partial skeleton of SMF-ME 11345A+B (Mayr, 2014b).
Hard minimum age. 47.0 Ma.
Minimum age justification. A maximum age for the fossiliferous deposits of the Messel Formation is provided by a 47.8 ± 0.2 Ma 40Ar/39Ar age obtained from the basalt chimney below Lake Messel (Mertz et al., 2004). This date provides a maximum age for Lake Messel itself, but a minimum age for the fossil must take into account time elapsed between the cooling of the basalt and the deposition of the fossiliferous layers that occur higher in the section. Lacustrine sediments are estimated to have filled in the maar lake that formed above this basalt chimney over a span of approximately 1 Ma (Mertz et al., 2004). Accounting for sedimentation rate, the layers yielding avian fossils (including SMF-ME 1883a+b) are most likely ~47 Ma in age (Mertz et al., 2004; Franzen, 2005). The Messel Formation has also yielded the stem hummingbird †*Parargornis messelensis* (Mayr, 2003), providing further support for this minimum constraint. Ksepka and Clarke (2015) recommended the slightly older †*Scaniacypselus wardi* at 51 Ma as a minimum calibration. We do not dispute this fossil's phylogenetic placement, but opted to use the slightly younger but more complete †*S. szarskii* specimen as a more conservative minimum.
Soft maximum age. 66.5 Ma.
Maximum age justification. The latest Cretaceous is set as the soft maximum, corresponding to the age range of the oldest known crown bird †*Vegavis*. No members of the nightbird–swift–hummingbird clade Strisores (to which Apodiformes

belong) are known from Cretaceous deposits, indicating it is unlikely the highly nested divergence between hummingbirds and swifts occurred before the Paleocene.

NODE CALIBRATED: AUSTRODYPTORNITHES (SPHENISCIFORMES + PROCELLARIIFORMES)
Fig. 2, node 35.

Prior shape. Approximate lognormal.

Fossil specimen. †*Waimanu manneringi* (CM zfa35).

Phylogenetic justification. Phylogenetic analysis supports the placement of †*Waimanu manneringi* along the penguin stem lineage (e.g., Ksepka et al., 2006; Slack et al., 2006). CM zfa35 is the only described specimen of †*W. manneringi*.

Hard minimum age. 60.5 Ma.

Minimum age justification. CM zfa35 was collected from the basal Waipara Greensand (Slack et al., 2006). Biostratigraphic evidence, specifically the ranges of *Hornibrookina teuriensis* and *Chaismolithus bidens*, indicates the minimum possible age of the fossil is 60.5 Ma (Cooper, 2004; Slack et al., 2006; Ogg et al., 2008).

Soft maximum age. 72.1 Ma.

Maximum age justification. The soft maximum is based on the lower bound of the Maastrichtian stage (Late Cretaceous). Southern Hemisphere Maastrichtian marine vertebrate sites have yielded diving birds such as †*Polarornis* and hesperornithids, indicating preservation potential for marine diving birds, but no penguin (or procellariiform) remains have been recovered at these sites.

NODE CALIBRATED: SULIFORMES (FREGATIDAE + SULIDAE + PHALACROCORACOIDEA)
Fig. 2, node 39.

Prior shape. Approximate lognormal.

Fossil specimen. †*Limnofregata azygosternon* (USNM 22753).

Phylogenetic justification. Phylogenetic analysis supports the placement of †*Limnofregata* as the sister taxon to extant *Fregata* (Smith, 2010), in agreement with long-standing interpretations of this fossil taxon (Olson, 1977). USNM 22753 is an articulated skeleton preserving most key synapomorphies that place †*L. azygosternon* on the frigatebird stem lineage.

Hard minimum age. 51.57 Ma.

Minimum age justification. USNM 22753 was collected from the Fossil Butte Member of the Green River Formation in Wyoming, U.S.A. The minimum date of 51.57 Ma incorporates the error associated with an $^{40}Ar/^{39}Ar$ date of 51.66 ± 0.09 Ma obtained from a potassium-feldspar (K-spar) tuff above the fossiliferous horizon containing USNM 336484 (Smith et al., 2008).

Soft maximum age. 66.5 Ma.

Maximum age justification. The latest Cretaceous is set as the soft maximum, corresponding to the age range of the oldest known crown bird †*Vegavis*. No members of the core waterbird clade Aequornithes (to which Suliformes belong) are known from Cretaceous deposits, indicating it is unlikely the highly nested divergence between frigatebirds and other Suliformes occurred before the Paleocene.

NODE CALIBRATED: PHALACROCORACOIDEA (ANHINGIDAE + PHALACROCORACIDAE)
Fig. 2, node 41.

Prior shape. Uniform.

Fossil specimen. †*Oligocorax* (= *Borvocarbo*) *stoeffelensis* (PW 2005/5022-LS).

Phylogenetic justification. The phylogenetic analysis of Smith (2010) recovered †*Oligocorax stoeffelensis* nested within Phalacrocoracoidea and more closely related to Phalacrocoracidae than to Anhingidae, whereas a phylogenetic analysis by Mayr (2015) recovered two alternate topologies, one placing †*O. stoeffelensis* as stem member of Phalacrocoracidae and one placing this fossil taxon within crown Phalacrocoracidae. Given the uncertainty, we conservatively place this calibration at the node representing the split between Phalacrocoracidae and Anhingidae. PW 2005/5022-LS preserves a substantial portion of the skeleton, including synapomorphy-bearing elements that support placement to at least the stem lineage of Phalacrocoracidae.

Hard minimum age. 24.52 Ma.

Minimum age justification. PW 2005/5022-LS was collected from the Enspel locality at Bad Marienberg in Westerwald, Rheinland-Pfalz, Germany (Mayr, 2007). Radiometric dating of basaltic flows that bound the Enspel deposits yielded ages of 24.56 ± 0.04 Ma (Mertz et al., 2007).

Soft maximum age. 52 Ma.

Maximum age justification. The soft maximum is based on the age of the oldest reported specimens assigned to Suliformes (the clade including Phalacrocoracoidea, Sulidae, and Fregatidae), which belong to the stem frigatebird †*Limnofregata* from the Early Eocene Green River Formation. No stem or crown Sulariformes are known from beyond this date.

NODE CALIBRATED: UNNAMED CLADE (ARDEIDAE + THRESKIORNITHIDAE)
Fig. 2, node 44.

Prior shape. Approximate lognormal.

Fossil specimen. †*Rhynchaeites* sp. indet. (MGUH 20288).

Phylogenetic justification. Multiple apomorphies support the placement of †*Rhynchaeites* within the Threskiornithidae (Mayr & Bertelli, 2011). Although the characteristic ibis-type bill is not preserved in MGUH 20288, derived characteristics of the hindlimb support assignment to †*Rhynchaeites* as well as placement along the stem lineage of Threskiornithidae (Mayr & Bertelli, 2011).

Hard minimum age. 53.9 Ma.

Minimum age justification. MGUH 20288 was collected from the Fur Formation of Denmark. The minimum age is based on a 54.04 ± 0.14 Ma radiometric date reported for layer +19 of the Fur Formation (Chambers et al., 2003).

Soft maximum age. 66.5 Ma.

Maximum age justification. The latest Cretaceous is set as the soft maximum, corresponding to the age range of the oldest known crown bird †*Vegavis*. No members of the core waterbird clade Aequornithes (to which Threskiornithidae belongs) are known from Cretaceous deposits, indicating it is unlikely the highly nested divergence between ibises and herons had occurred before the Paleocene.

NODE CALIBRATED: PELECANIFORMES (PELECANIDAE + BALAENICIPITIDAE)
Fig. 2, node 45.

Prior shape. Uniform.

Fossil specimen. *Pelecanus* sp. indet. (NT-LBR-039).

Phylogenetic justification. NT-LBR-039 is essentially identical to modern pelicans in cranial osteology and preserves multiple synapomorphies of Pelecanidae (Louchart et al., 2011).

Hard minimum age. 28.1 Ma.

Minimum age justification. NT-LBR-039 was collected from the Pichovet locality in Lubéron, France (Louchart et al., 2011). The fossil horizon is Rupelian in age (Oligocene), and

thus the upper boundary of the Rupelian stage is used as the hard minimum.

Soft maximum age. 53.9 Ma.

Maximum age justification. The soft maximum age is based on the age of the oldest members of Ciconiiformes s.l. (†*Rhynchaeites*, see above) and the absence of other convincing representatives of Pelecaniformes, Sulariformes, and Ciconiiformes in deposits older than 53.9 Ma.

NODE CALIBRATED: EUCAVITAVES (TROGONIDAE + PICOCORACIAE)
Fig. 2, node 55.

Prior shape. Approximate lognormal.

Fossil specimen. †*Septentrogon madseni* (MGUH VP3496).

Phylogenetic justification. Cranial characters including the mediolaterally flattened and rounded zygomatic processes, a synapomorphy of trogons, support placement of †*Septentrogon* to at least the trogon stem lineage (Kristoffersen, 2002).

Hard minimum age. 53.9 Ma.

Minimum age justification. MGUH VP3496 was collected from the Fur Formation of Denmark. The minimum age is based on a 54.04 ± 0.14 Ma radiometric date reported for layer +19 of the Fur Formation (Chambers et al., 2003).

Soft maximum age. 66.5 Ma.

Maximum age justification. The latest Cretaceous is set as the soft maximum, corresponding to the age range of the oldest known crown bird †*Vegavis*. No members of the higher landbird clade Telluraves (to which Trogoniformes belong) are known from Cretaceous deposits, indicating it is unlikely that the nested divergence of trogons from other landbirds had occurred before the Paleocene.

NODE CALIBRATED: UNNAMED CLADE (ALCEDINIDAE + CORACIOIDEA)
Fig. 2, node 60.

Prior shape. Approximate lognormal.

Fossil specimen. †*Primobucco mcgrewi* (USNM 336484).

Phylogenetic justification. Phylogenetic analyses place †*Primobucco mcgrewi* along the stem lineage leading to the clade Coracioidea (rollers and ground rollers) (Mayr et al., 2004; Clarke et al., 2009).

Hard minimum age. 51.57 Ma.

Minimum age justification. USNM 336484 was collected from the Middle unit of the Fossil Butte Member of the Green River Formation in Wyoming, U.S.A. The minimum date of 51.57 Ma incorporates the error associated with an $^{40}Ar/^{39}Ar$ date of 51.66 ± 0.09 Ma obtained from a potassium-feldspar (K-spar) tuff above the fossiliferous horizon containing USNM 336484 (Smith et al., 2008).

Soft maximum age. 66.5 Ma.

Maximum age justification. The latest Cretaceous is set as the soft maximum, corresponding to the age range of the oldest known crown bird †*Vegavis*. No members of the higher landbird clade Telluraves (to which Coraciiformes belong) are known from Cretaceous deposits, indicating it is unlikely the highly nested roller–kingfisher divergence had occurred before the Paleocene.

NODE CALIBRATED: PSITTACOPASSERAE (PSITTACIFORMES + PASSERIFORMES)
Fig. 2, node 63.

Prior shape. Approximate lognormal.

Fossil specimen. †*Pulchrapollia gracilis* (NHMUK A6207).

Phylogenetic justification. Phylogenetic analyses have consistently recovered †*Pulchrapollia gracilis* as a stem lineage parrot (Dyke & Cooper, 2000; Mayr, 2005b; Ksepka et al., 2011).

Hard minimum age. 53.5 Ma.

Minimum age justification. NMHUK A6207 was collected from the Walton Member (Division A2) of the London Clay Formation at Walton-on-the-Naze, England. The Walton Member correlates to the upper part of Chron C24r, and the minimum age is based on the youngest estimate for the top of C24r (53.54 ± 0.04) presented by Westerhold et al. (2007). Additional evidence for this minimum date is provided by the oldest reported Passeriformes, which are more fragmentary remains from the Early Eocene Murgon site of Australia (Boles, 1995, 1997).

Soft maximum age. 66.5 Ma.

Maximum age justification. The latest Cretaceous is set as the soft maximum, corresponding to the age range of the oldest known crown bird †*Vegavis*. No members of the higher landbird clade Telluraves (to which the Psittacopasserae belongs) are known from Cretaceous deposits, indicating it is extremely unlikely the highly nested parrot–songbird divergence had occurred before the Paleocene.

NODE CALIBRATED: EUPASSERES (TYRANNI + PASSERI)
Fig. 2, node 66.

Prior shape. Uniform.

Fossil specimen. SMNS 59466/1 (suboscine sp. indet.).

Phylogenetic justification. The presence of a distally protruding fingerlike process at the cranial edge of metacarpal III is an apomorphic feature supporting assignment of SMNS 59466/1 to at least the suboscine stem lineage.

Hard minimum age. 26 Ma.

Minimum age justification. SMNS 59466/1 was collected from the Herrlingen 11 locality at Ulm, Baden-Württemberg, Germany (Manegold, 2008). Szyndlar (1994) determined an age of Mammal Paleogene (MP) zones 28 to 30 for this locality, and Manegold (2008) indicated an age of MP 28 based on a personal communication from Bötticher. Thus, the lower age limit of MP 28 is used as a hard minimum age. Additional fossils from this site have been assigned to the oscine lineage, providing additional support for this constraint.

Soft maximum age. 55.0 Ma.

Maximum age justification. The oldest reported Passeriformes are from the Early Eocene Murgon site of Australia (Boles, 1995, 1997). These fossils bear primitive characters indicating they fall outside Eupasseres (Mayr, 2013). Furthermore, no crown Passeriformes are found in Eocene deposits, such as the Green River Formation and Messel Formation, which otherwise preserve an abundance of small birds. Thus, the age of the Murgon fossils is used a soft maximum.

APPENDIX 2. Sources for sequence data. All nuclear data for primary species follow Hackett et al. (2008). GenBank accession numbers for mitochondrial genomes are listed after the taxonomic identification. Other species names and accession numbers for genes were added to composite taxa to improve sequence representation. UTRs represent untranslated regions of nuclear DNA.

Primary species for nuclear loci	Matching mt genome	Taxa sampled to improve sequence representation
Acanthisitta chloris	*Acanthisitta chloris* (AY325307)	
Aegotheles insignis	*Aegotheles cristatus* (NC_011718)	
Aerodramus vanikorensis	*Apus apus* (NC_008540)	
Alcedo leucogaster	*Todiramphus sanctus* (NC_011712)	*Momotus momota* ALDOB (EU737869), NGFB (EU740156), MUSK (EU739836), *Todus angustirostris* EGR1 [exons only] (EU739036), NTF3 (EU740377)
Alectura lathami	*Alectura lathami* (AY346091)	*Megapodius eremita* FGB [exons only] (EU739436)
Anas platyrhynchos	*Anas falcata* (KC759527)	
Anhinga anhinga	*Anhinga rufa* (NC_014681)	
Anser erythropus	*Anser albifrons* (AF363031)	
Anseranas semipalmata	*Anseranas semipalmata* (AY309455)	
Apteryx australis	*Apteryx mantelli* (AY016010)	
Ardea herodias	*Ardea novaehollandiae* (NC_008551)	
Arenaria interpres	*Arenaria interpres* (NC_003712)	
Aythya americana	*Aythya americana* (NC_000877)	
Balaeniceps rex	*Balaeniceps rex* (GU071053)	
Bucorvus abyssinicus	*Bucorvus leadbeateri* (NC_015199)	
Buteo jamaicensis	*Buteo buteo* (AF380305)	
Cacatua sulphurea	*Cacatua moluccensis* (JF414239)	
Casuarius casuarius	*Casuarius casuarius* (AF338713)	
Cathartes aura	*Cathartes aura* (AY463690)	
Chalcopsitta cardinalis	*Melopsittacus undulatus* (NC_009134)	
Ciconia ciconia	*Ciconia ciconia* (NC_002197)	
Colibri coruscans	*Archilochus colubris* (NC_010094)	*Colibri coruscans* FGB (EU739462)
Columba livia	*Columba livia* (NC_013978)	*Geotrygon montana* TPM1 (EU737540)
Coracias caudata	*Eurystomus orientalis* (EU344978)	*Brachypteracias squamigera* CRYAA (EU737653), MUSK [exons only] (EU739772)
Corvus corone	*Corvus frugilegus* (NC_002069)	
Coturnix coturnix	*Coturnix japonica* (NC_003408)	
Crotophaga sulcirostris	*Crotophaga ani* (HM746794)	
Crypturellus soui	*Crypturellus tataupa* (AY016012)	
Cuculus canorus	*Eudynamys taitensis* (EU410487)	*Coccyzus americanus* RHO (EU737195), FBG [exons only] (EU739390), MYC (EU738272), MUSK [exons only] (EU739786)
Diomedea nigripes	*Thalassarche melanophris* (AY158677)	
Dromaius novaehollandiae	*Dromaius novaehollandiae* (NC_002784)	
Dryocopus pileatus	*Dryocopus pileatus* (NC_008546)	*Indicator maculatus* ALDOB (EU737855), RHO (EU737230)
Eudocimus albus	*Nipponia nippon* (NC_008132)	
Eudromia elegans	*Eudromia elegans* (NC_002772)	
Eudyptula minor	*Eudyptula minor* (AF362763)	
Eupodotis ruficrista	*Otis tarda* (NC_014046)	*Choriotis kori* [= *Ardeotis kori*] EEF2 (EU738599)
Falco mexicanus	*Falco peregrinus* (AF090338)	*Daptrius ater* MUSK [exons only] (EU739799)
Fregata magnificens	*Fregata* sp. (AP009192)	
Fringilla montifringilla	*Taeniopygia guttata* (DQ422742)	*Passer montanus* FGB (EU739142, EU739290, EU739455)
Gallus gallus	*Gallus gallus* (GU261713)	
Gavia immer	*Gavia stellata* (NC_007007)	
Geococcyx californianus	*Geococcyx californianus* (EU410488)	
Grus canadensis	*Grus grus* (NC_020577)	*Aramus guaranus* RHO (EU737173)
Haematopus ostralegus	*Haematopus ater* (AY074886)	
Larus marinus	*Larus dominicanus* (AY293619)	
Megalaima virens	*Pteroglossus azara* (NC_008549)	*Capito niger* TGFB2 [exons only] (EU737344), EEF2 [exons only] (EU738591)
Menura novaehollandiae	*Menura novaehollandiae* (NC_007883)	

Appendix 2. Continued.

Primary species for nuclear loci	Matching mt genome	Taxa sampled to improve sequence representation
Micrastur semitorquatus	*Micrastur gilvicollis* (NC_008548)	*Herpetotheres cachinnans* TGFB2 [exons only] (EU737391), EGR1 [exons only] (EU738961), FGB (EU739118, EU739266, EU739427), MUSK (EU739821)
Morus bassanus	*Morus serrator* (GU071056)	
Numida meleagris	*Numida meleagris* (NC_006382)	
Nyctibius grandis	*Nyctibius grandis* (EU344977)	*Nyctibius bracteatus* EEF2 (EU738651)
Oceanites oceanicus	*Pelagodroma marina* (KC875856)	
Pandion haliaetus	*Pandion haliaetus* (NC_008550)	
Pelecanus occidentalis	*Pelecanus conspicillatus* (DQ780883)	
Phaethon rubricauda	*Phaethon rubricauda* (NC_007979)	*Phaethon lepturus* CRYAA (EU737730), MUSK (EU739852)
Phalacrocorax carbo	*Phalacrocorax chalconotus* (NC_014679)	
Phoenicopterus chilensis	*Phoenicopterus roseus* (NC_010089)	
Podiceps auritus	*Tachybaptus novaehollandiae* (EF532936)	
Puffinus griseus	*Pterodroma brevirostris* (AY158678)	
Rallus limicola	*Porphyrio hochstetteri* (NC_010092)	*Sarothrura elegans* TPM1 (EU737596), *Himantornis haematopus* MUSK (EU739822)
Rhea americana	*Rhea americana* (AF090339)	
Rhynochetos jubatus	*Rhynochetos jubatus* (NC_010091)	*Eurypyga helias* EEF2 [introns/UTRs only] (EU738789), FGB (EU739107, EU739253, EU739413)
Smithornis rufolateralis	*Smithornis sharpei* (NC_000879)	*Pitta guajana* TPM1 (EU737582), EGR1 [introns/UTRs only] (EU738843)
Strix occidentalis	*Ninox novaeseelandiae* (NC_005932)	*Speotyto cunicularia* CRYAA (EU737757), FGB [exons only] (EU739490)
Struthio camelus	*Struthio camelus* (AF338715)	
Sylvia nana	*Sylvia crassirostris* (NC_010229)	
Tinamus guttatus	*Tinamus major* (NC_002781)	
Tockus camurus	*Aceros corrugatus* (HM755883)	
Trogon personatus	*Trogon viridus* (NC_011714)	
Tyrannus tyrannus	*Cnemotriccus fuscatus* (NC_007975)	*Mionectes macconnelli* MB (EU739991)
Tyto alba	*Tyto alba* (EU410491)	*Phodilus badius* RHO (EU737263)
Vidua chalybeata	*Vidua chalybeata* (AF090341)	

APPENDIX 3. Body mass estimates for internal nodes representing pairs of tip taxa, based on species data from the CRC Handbook of Avian Masses (Dunning, 2008). Species means were used, and when sequences were taken from multiple taxa (see Appendix 2), all sampled species were included in the average for that composite taxon. Node numbers correspond to those shown in Figure 2.

Node	Taxa included in comparison	Average body mass (g)
6. Casuariiformes	*Dromaius novaehollandiae*, *Casuarius casuarius*	391,000.0
8. *Crypturellus/Tinamus*	*Crypturellus soui*, *Crypturellus tataupa/Tinamus major*, *Tinamus guttatus*	534.7
13. *Gallus/Coturnix*	*Gallus gallus/Coturnix coturnix*, *Coturnix japonica*	467.3
16. *Anas/Aythya*	*Anas platyrhynchos*, *Anas falcata/Aythya americana*	1081.9
20. Mirandornithes	*Podiceps auritus*, *Tachybaptus novaehollandiae/Phoenicopterus chilensis*, *Phoenicopterus roseus*	1501.1
21. Columbiformes/Phaethontiformes	*Columba livia/Phaethon rubricauda*, *Phaethon lepturus*	507.1
25. Apodiformes	*Aerodramus vanikorensis*, *Apus apus/Colibri coruscans*, *Archilochus colubris*	14.6
31. *Geococcyx/Crotophaga*	*Geococcyx californianus/Crotophaga sulcirostris*, *Crotophaga ani*	238.3
32. Grues/Rallidae	*Grus canadensis*, *Grus grus*, *Aramus guaranus/Rallus limicola*, *Porphyrio hochstetteri*, *Sarothrura elegans*, *Himantornis haematopus*	1877.8
37. *Puffinus/Diomedea*	*Puffinus griseus*, *Pterodroma brevirostris/Diomedea nigripes*, *Thalassarche melanophris*	1967.2
41. Phalacrocoracoidea	*Phalacrocorax carbo*, *Phalacrocorax chalconotus/Anhinga anhinga*, *Anhinga rufa*	1429.1
44. Ardeidae/Threskiornithidae	*Ardea herodias*, *Ardea novaehollandiae/Eudocimus albus*, *Nipponia nippon*	1404.5
45. *Pelecanus/Balaeniceps*	*Pelecanus occidentalis*, *Pelecanus conspicillatus/Balaeniceps rex*	5018.7
48. *Arenaria/Larus*	*Arenaria interpres/Larus marinus*, *Larus dominicanus*	727.9
51. *Buteo/Pandion*	*Buteo jamaicensis*, *Buteo buteo/Pandion haliaetus*	1242.7
53. Strigiformes	*Strix occidentalis*, *Ninox novaeseelandiae*, *Speotyto cunicularia/Tyto alba*, *Phodilus badius*	323.3
57. Bucerotiformes	*Bucorvus abyssinicus*, *Bucorvus leadbeateri/Tockus camurus*, *Aceros corrugatus*	437.7
59. Pici	*Megalaima virens*, *Pteroglossus azara*, *Capito niger/Dryocopus pileatus*, *Indicator maculatus*	151.9
60. Alcedinidae/Coracioidea	*Alcedo leucogaster*, *Todiramphus sanctus*, *Momotus momota*, *Todus angustirostris/Coracias caudata*, *Eurystomus orientalis*, *Brachypteracias squamigera*	26.7
62. Falconidae	*Falco mexicanus*, *Falco peregrinus*, *Daptrius ater/Micrastur semitorquatus*, *Micrastur gilvicollis*, *Herpetotheres cachinnans*	496.3
64. Psittaciformes	*Chalcopsitta cardinalis*, *Melopsittacus undulatus/Cacatua sulphurea*, *Cacatua moluccensis*	312.0
67. Tyranni	*Smithornis rufolateralis*, *Smithornis sharpei*, *Pitta guajana/Tyrannus tyrannus*, *Mionectes macconnelli*	36.1
71. *Vidua/Fringilla*	*Vidua chalybeata/Fringilla montifringilla*, *Passer montanus*, *Taeniopygia guttata*	16.7